Perovskites for Solar and Thermal Energy Harvesting: State of the Art Technologies, Current Scenario and Future Directions

Richa Pandey^{a,b, #}, Gaurav Vats^{c,#,*}, Jae Yun^d, Chris R Bowen^e, Anita W. Y. Ho-Baillie^d and Jan Seidel^c

^aCentre of Excellence in Nanoelectronics, Indian Institute of Technology Bombay, Powai 400076, India

^bCentre for Research in Nanotechnology and Science, Indian Institute of Technology Bombay, Powai 400076, India

^cSchool of Materials Science and Engineering, University of New South Wales, Sydney 2052, Australia

^dAustralian Centre for Advanced Photovoltaics, School of Photovoltaic and Renewable Energy Engineering

^eMaterials Research Centre, Department of Mechanical Engineering, University of Bath, Bath BA2 7AY, United Kingdom

^{*}Email: er.gauravvats17@gmail.com, g.vats@student.unsw.edu.au; Phone: +61 481354339

[#]Authors contributed equally.

Abstract:

Solar energy is anticipated to be the most viable source of sustainable green energy. Perovskites have gained significant research attention in recent years as a solar energy harvesting material due to their desirable photovoltaic enabling properties. The potential strategies for a more effective use of these materials can involve multiple energy conversion mechanisms through a single device or employing materials where a solar or thermal input provides multiple electrical outputs to enhance the overall energy harvesting capability. In this context, the present review focuses on perovskites, including both organic halide perovskites and inorganic oxide perovskites, due to their proven properties as photovoltaic materials and their intriguing potential for additional functionality, such as ferroelectricity. Ferroelectrics are a special class of perovskites that have been studied in detail for photoferroic, pyroelectric and thermoelectric effects and energy storage, which we briefly review here. Furthermore, the possibilities of simultaneously tuning these mechanisms in perovskite materials for multiple energy conversion mechanisms and storage for ultra-high density capacitor and battery applications is also examined in order to attain a better understanding and to present novel opportunities. An understanding of all these mechanisms and device prospects will inspire and inform the selection of appropriate materials and potential novel designs so that the available solar and thermal resource could be utilized in a more effective manner. This review will not only help in selecting an appropriate material from the existing pool of perovskite materials, but will also provide an outlook and assistance to researchers in developing new material systems.

Keywords: Photovoltaics, perovskites, photoferroic effect, pyroelectric effect, energy harvesting, ferroelectrics, thermo-electric effect, energy storage, batteries, capacitors, materials selection.

1. Introduction

The Kyoto Protocol initiative to reduce carbon emission has endorsed solar energy as the most viable source of sustainable green energy^{1, 2}. In this context, solar cells have been deployed faster than anticipated³ and the solar cell market is expected to exceed a 100 billion USD milestone by 2024; as highlighted in competitive market share and forecast report (2016-2024). In addition, the International Energy Agency (IEA) has anticipated an annual investment of 225 billion USD to achieve power generation levels of 124-200 GW per year using photovoltaic cells and an installed capacity of 4600 GW by 2050 in order to avoid the emission of four gigatonnes of CO₂ annually and restrict the mean global temperature rise to 2°C, rather than a predicted 6°C¹. Major efforts have been dedicated to reduce the cost and enhance the efficiency of photovoltaics. In this context, novel materials are constantly being explored. Among these materials perovskites have gained significant research interest in recent years because of their low cost and ease of production via soft chemistry⁴⁻⁹. *Perovskites* are materials with a ABX₃ type structure where cation 'A' occupies the corner positions of the unit cell, cation 'B' is situated at the center of the cell, and anion 'X' is located at the faces of the unit cell; see Figure 1(a) and (b). Perovskites can be classified based on their band gaps as conductors and insulators/dielectrics. Dielectrics with a band gap less than 3eV are termed semiconductors. These can also be classified as centrosymmetric, asymmetric and non-centrosymmetric based on their symmetry.

<Figure 1>

Figure 1: (a) Perovskite structure with symmetric and (b) non-centrosymmetric arrangements. (b)-(c) tuning of the degree of non-centrosymmetry by means of an external stimulus, where *E* is

electric field, T is temperature, hv is the photon energy (h is the Planck's constant and v is the frequency of the incident light) and σ is the stress.

Figure 2 indicates the classification scheme for perovskites and highlights the domain of interest of this Perspective Paper. The figure indicates that a perovskite can be any material with ABX₃ type structure, while ferroelectrics are restricted to the non-centrosymmetric dielectric or semi-conducting materials that possess a spontaneous polarization which can be fully switched by application of an external electric field, stress, thermal fluctuation or light, as illustrated in Figure 1 (b)-(c). The phenomena of achieving a switchable polarization by means of thermal fluctuations is known as the 'pyroelectric effect' while switching of polarization by exposure of light or stress is termed as 'photoferroic effect' and 'piezoelectric effect' respectively. It is to be noted that all ferroelectrics are both pyroelectric and piezoelectric in nature, while the reverse is not true. Figure 3 provides an insight into the relationship between these materials and suggests that a single material could have the desired multiple functionalities which could be utilized simultaneously. Thus, it will be of interest to explore the possibilities of simultaneously harnessing energy from different sources and distinct mechanisms using a single perovskite material, since hybrid perovskites have already been established for photovoltaic⁴⁻⁹ applications and current research is focused on understanding their behavior on the basis of their crystal structure so that better materials can be developed and designed ¹⁰⁻¹².

<Figure 2>

Figure 2: Classification of perovskites for thermal energy harvesting based on their band gap and crystal symmetry.

In addition, ferroelectrics, a special class of perovskites, are already well known for piezoelectric, pyroelectric and thermal energy conversion systems¹³⁻³⁹, and are also gaining interest as photovoltaic materials⁴⁰⁻⁵¹. Intriguingly, both hybrid perovskites and ferroelectrics are also being investigated for thermoelectric applications^{52, 53}. Therefore, the possibilities of utilizing this class of materials to provide multiple functionalities for a more desirable energy output is worthy of consideration. Often, these approaches are considered entirely different branches of research, however considering them simultaneously and holistically can provide several new opportunities. This requires a basic understanding of concepts, mechanisms, corresponding material properties and the underlying physics involved with these different effects. In this context, this perspective aims to provide an understanding of these phenomena as well as state-of-the-art research to motivate researchers from distinct backgrounds and provide pathways to develop better materials systems and devices. The article begins with the basics of solar cells and leads to the emergence of perovskite solar cells. It is then followed by a discussion of photoferroics, pyroelectric energy harvesting, thermo-electric energy conversion and energy storage using supercapacitors and batteries. Finally, the possibilities of coupled mechanisms/devices and future prospects are discussed.

<Figure 3>

Figure 3: Relationships between perovskite, piezoelectric, pyroelectric and ferroelectric materials

2. The Evolution of Solar Cells

Silicon solar cells currently make up for 93% of photovoltaic products of which more than 95% are based on a p-n junction architecture⁵⁴. A silicon p-n junction solar cell produces power by

absorbing light to generate electron-hole pairs followed by the separation of charge carriers by the p-n junction and the collection of the electrons (in the n-type material as the majority carrier) and holes (in the p-type material as the majority carrier) by the electrodes. Figure 4 demonstrates the working principle of a simple p-n junction solar cell. The power conversion efficiency (η) of these cells is expressed as the ratio of output electrical power (P_{out}) to the input solar energy (P_{in}) absorbed. From the short circuit, current density (J_{sc}) and the open circuit voltage (V_{oc}), the efficiency can be calculated^{55, 56}:

$$\eta = \frac{P_{out}}{P_{in}} = \frac{J_{sc}V_{oc}FF}{P_{in}}; \text{ FF} = \frac{P_{out}}{J_{sc}V_{oc}}$$
(1)

where, FF is the *fill factor* and is defined as the ratio of the maximum obtainable power to the product of short circuit current density (J_{sc}) and the open circuit voltage (V_{oc}) and is limited by parasitic losses such as carrier recombination at the surface and within the bulk, series and shunt resistances. The timeline for development of solar cells can generally be distinguished by the first, second and third generation of solar cells. First-generation solar cells are made of crystalline silicon which dominates the current market. Second-generation cells are typically thin-film photovoltaic cells and despite being an attractive alternative, they come at the expense of a reduced efficiency and contribute to only 7% of the market in 2015. Third-generation of solar cells employ more futuristic concepts and materials including those that utilize electrostatically bound electrons and holes known as *excitons*. In contrast to the directly generated electron-hole pairs in conventional *p-n* junction solar cells these systems have low binding energy and hence induce more current by utilizing photons with comparatively less energy⁵⁷. Third-generation solar cells can further be sub-categorized in organic photovoltaic

cells with planar interfaces (OPCPI), organic photovoltaic heterojunction cells (OPHC) and dyesensitized solar cells (DSSC). OPCPI cells employ an organic polymer that is sandwiched
between two metal electrodes with different work functions to confine excitons for light
absorption and current generation⁵⁷. These cells have low quantum efficiency, which was later
overcome by the development of OPHC cells. Unlike the single polymer layer in OPCPI devices,
OPHC cells have two organic layers with a different ionization energy⁵⁸ which provides an
additional electric potential across the heterostructure and aids in breaking excitons. However,
the typical diffusion length of excitons in organic materials is small (on the order of ~10 nm),
while a 100 nm absorber thickness is required to produce a sufficient number of excitons. Due to
this difference in diffusion length and absorber thickness most of the excitons disappear before
reaching the heterojunction and hence merely provide a small contribution towards current
generation⁵⁸. This deficiency has encouraged the development of dispersed organic photovoltaic
cells and the concept was extensively used in DSSC.

<Figure 4>

Figure 4: Working principle of a basic p-n junction solar cell.

DSSCs have gained popularity as a potential low-cost photovoltaic alternative ^{4, 6, 59}. The advantage of these cells is that they employ different materials for light absorption and electron and hole transportation. This not only makes these solar cells unique, but it also provides opportunities to tune the performance of these cells by developing new cell materials, cell designs and new cell architectures.

<Figure 5>

Figure 5: Energy level and device operation of a DSSC. Reproduced from Ref: ⁶, © 2012 Macmillan Publishers Limited.

The materials for such cells typically consist of wide band gap mesoporous semiconductors of high surface area, such as TiO₂, ZnO or SnO₂, which are sensitized with a nano-crystalline dye and anchored within a hole-conducting electrolyte or within a hole-transport material (HTM). The system is then sandwiched between two electrodes, one of which is transparent, which is further encapsulated with a glass layer. On exposure to sunlight, the dye absorbs light and a photoexcited electron transfers to the conduction band of the semiconductor and is finally carried to one of the electrodes⁶⁰. Typically, a redox couple transports the positive charge to the other electrode by reducing the oxidized dye to its neutral state^{6, 61}. Figure 5 shows the energy level diagram and device operation principle of a typical DSSC. where initially the sensitizing dye absorbs a photon of energy, *hv*, and consequently an electron is injected into the conduction band of the metal oxide; in this case titania. Thereafter, the electron travels to the front electrode (not shown). In addition, the oxidized dye is reduced by the electrolyte, which is regenerated at the counter-electrode to complete the circuit (not shown).

The first DSSC was introduced by O'Regan and Grätzel in 1991⁵⁹ for which the overall light-to-electric energy conversion yield was 7.1-7.9% in simulated solar light and 12% in diffuse daylight. Initial complications associated with electrolyte leakage in this cell were later resolved by substituting the liquid electrolyte with a solid hole conductor ^{62, 63}, and such cells are known as solid-state DSSC (ssDSSC). Further progress in the field of DSSCs realized the significance of using ruthenium based organometallic complex sensitizers^{64, 65} and an iodide/tri-iodide redox couple ^{10,11}. The iodide/tri-iodide redox couple provided reduced recombination kinetics which

led to longer electron lifetimes of up to 1 s ⁶⁶⁻⁶⁸. Unfortunately, this system is highly corrosive which has an impact on any metal interconnects and sealants in manufactured devices⁶. These developments led to an improved understanding and to a large increase in the efficiency of DSSCs in the late 1990s, which approached approximately 11.5% in 2006 ⁶⁹⁻⁷¹.

3. The Emergence of Perovskite Solar Cells

Perovskite solar cells have emerged as an advancement of the DSSC^{7-9, 72}. Previous parallel research efforts on organic-inorganic hybrids for light emitting diodes (LED) and transistors^{73, 74} were anticipated to be applied to solar cell applications by Mitzi and co-workers⁷⁴. However, this did not gain significant attention, which is possibly due to environmental issues associated with the use of lead (Pb) and concerns regarding the robustness of tin (Sn) based perovskites⁸. However, the first reports on the photovoltaic response of organometallic perovskites are attributed to Miyasaka's group with documented efficiencies of 2.2% (2006) and 3.8% (2009) in CH₃NH₃PbBr₃ and CH₃NH₃PbI₃ respectively⁷⁵⁻⁷⁷. Thereafter, Park and co-workers (2011) achieved an efficiency of 6.5% by optimizing the perovskite coating solution concentration, postannealing condition and TiO₂ surface modification⁷⁸. Although the performance of their perovskite sensitizers ((CH₃NH₃)PbI₃ quantum dots) was better than the standard N719 dye sensitizers, they possessed a poor stability and dissolved in the electrolyte under continuous irradiation after only 10 minutes⁷⁸. In order to address their stability, the Park and Grätzel groups combined efforts for the replacement of the electrolyte by a solid-state hole transport material, (2,2',7,7'-tetrakis(N,N-di-p-methoxyphenylamine)-9,9'namely spiro-MeOTAD spirobifluorene)⁷⁹. This not only enhanced the stability of the cell, but also improved the efficiency to 9.7%⁷⁹. In the same year (2012), Snaith and colleagues introduced four additional developments along with spiro-MeOTAD and reported an efficiency of 10.9% 80. Further efforts

considered the following aspects (a) the use of mixed halide CH₃NH₃PbI_{3-x}Cl_x to achieve an improved stability and carrier transport in contrast to pure iodide and bromide equivalents^{80, 81}; (b) forming an extremely thin absorber (ETA) by coating a thin perovskite layer onto TiO₂; (c) replacing the conducting nano-porous TiO₂ with a non-conducting Al₂O₃ network; (d) utilizing ambipolar transport by aid of planar cells without any scaffolding^{8, 80}. This work exploited the fact that perovskites are capable of transporting both electron and holes to the cell terminals, rather than merely working as sensitizers⁸. In 2013, Seok and Grätzel introduced a polymeric hole conductor (poly-triarylamine) with a three-dimensional nanocomposite of mesoporous-TiO₂ and CH₃NH₃PbI₃ perovskite as the light harvester⁸². This led to a power conversion efficiency of 12.0%, with a substantial improvement in the open circuit voltage and fill factor of the cell⁸². Seok and co-workers replaced CH₃NH₃PbI₃ with CH₃NH₃PbI_{3-x}Br_x and raised the efficiency further to 12.3%83 which was followed by attempts to attain a better morphology of the perovskite layer for improved efficiency. This included the use of sequential deposition in which the initial PbI₂ solution was introduced into a nanoporous titanium dioxide film and later exposed to CH₃NH₃I for transformation into CH₃NH₃PbI₃ perovskite⁸⁴. Similarly, a mixed halide (CH₃NH₃PbI_{3-x}Cl_x) was deposited by a two-source thermal evaporation and an efficiency of 15.4% was achieved⁸⁵. By the end of 2013, the efficiency approached 16.2% using a mixed halide CH₃NH₃PbI_{3-x}Br_x (10-15% Br) and a poly-triarylamine HTM⁸⁶. In 2014, a confirmed efficiency of 17.9% was reported by mixing the lower bandgap CH(NH₂)₂PbI₃ with the CH₃NH₃PbBr₃ as the light-harvesting layer⁸⁷, there was also an unconfirmed efficiency of 19.3%^{8, 88}. Zhou et. al. fabricated CH₃NH₃PbI₃ perovskite on doped TiO₂ with an yttrium and modified indium tin oxide cathode with polyethylenimine ethoxylated to reduce the contact barrier⁸⁹. An efficiency of 20.1% was independently confirmed in late 2014, as demonstrated by

Seok and co-workers⁹⁰. In this work, high-quality FAPbI₃ films were fabricated by direct intramolecular exchange of dimethylsulfoxide (DMSO) molecules intercalated in PbI₂ with formamidinium iodide. To date, the highest reported efficiency for a perovskite solar cells is at 22.1%, demonstrated by the team at the Korea Research Institute of Chemical Technology (KRICT) and Ulsan National Institute of Science and Technology (UNIST)⁹¹. Recent work further extended the efficiency to 23.6% by employing a two-terminal tandem configuration using an infrared-tuned silicon heterojunction bottom cell and a caesium formamidinium lead halide perovskite top cell ⁹². Figure 6 summarizes the progress to date and provides an insight into the existing DSSC and perovskite solar cells.

<Figure 6>

Figure 6: Timeline for the evolution of perovskite solar cells; beginning with the discovery of (a) a DSSC which was comprised of a liquid electrolyte and dye sensitized mesoscopic TiO_2^{59} . Electrolyte leakage was eliminated by introducing a solid state organic p-type hole conductor ((b) ssDSSC)^{62, 63}. Later, in (c) extremely thin absorber (ETA) cells replaced the dye with an extremely thin absorber semiconductor layer^{93, 94}. The efficiency was further improved in (d) meso-superstructured solar cell (MSSC) by using a perovskite layer and a porous insulating scaffold instead of an ETA and TiO_2 respectively⁸⁰. It is suggested that the efficiency is likely to improve by employing (e) porous perovskite p-n heterojunctions⁷ and (f) p-i-n thin film perovskite solar cells in which a thin perovskite film is sandwiched between p-type and n-type charge-extracting contacts ^{7, 95, 96}.

At this stage, it is important to note that unlike DSSCs, perovskite solar cells utilize a single perovskite layer for both light absorption and electron-hole transportation. However, a barrier to

commercial deployment of these materials is their poor stability and the toxicity of lead in the most efficient perovskite cells ^{97, 98}. In this context, Giustino and Snaith have provided an insight on various possible lead-free alternatives, which are shown in Table 1 of reference 9. However, the continued investigation and search for improved materials is warranted as the efficiency achieved using lead-free counterparts remains relatively low. Recently, Wang et. al. reported a potential restriction on further progress in iodide based perovskite cells⁹⁹. They revealed that iodide based perovskites produced gaseous iodine (I₂) during operation, which has a high vapor pressure and therefore permeates through the perovskite layer and results in degradation of the material⁹⁹. However, they did not completely rule out the possibility of using iodide perovskites for solar cells, but strongly advocated the need to develop new stable perovskites. Recently, Shin et. al. employed inorganic perovskite, La doped BaSnO₃, as an electron transport layer instead of a conventional TiO₂ and achieved a remarkable efficiency of 21.2% and photostability¹⁰⁰. It retains 93% of its initial performance after 1,000 hours of exposure to sunlight. 100 In addition, parallel research is ongoing to understand the existence and possibility of ferroelectricity¹⁰¹⁻¹⁰⁴ in such materials which is often overlooked and has also become a question of debate in recent vears¹⁰⁵⁻¹⁰⁹. Interestingly, inorganic ferroelectric materials are also being explored for solar energy harvesting and the effect is known as photo-ferroelectric/photoferroic or ferroelectric photovoltaic^{42-45, 110-114}.

4. Ferroelectric Photovoltaics and Photoferroics

Polar materials are being extensively studied as a potential alternative to semiconductor-based materials for photovoltaic applications^{40, 41, 46, 49, 115-122}. The dipole moment in these materials due to exposure to light, heat or by inducing an internal field and interface band bending when an external voltage is applied to the system facilitates the generation of charge carriers at the

material-electrode interface. Among these materials, ferroelectrics have additional advantages such as piezo- and pyro-electricity, as described in Section 1. Research in this area started with the discovery of the generation of a photocurrent in paraelectric BaTiO₃¹²³, this was followed by the detection of above band gap photovoltages in cadmium telluride¹²⁴⁻¹²⁶ and zinc sulfide thin films¹²⁷. Later, in the early 1970s, a bulk or anomalous photoferroic/photovoltaic effect was discovered in non-centrosymmetric crystals; this is also known as the galvanic effect or nonlinear photonics^{43, 51}. This effect in ferroelectric and multi-ferroic materials refers to the phenomena of obtaining a steady state current in short circuit condition or a high output photovoltage in the open circuit condition in the direction of polarization of the materials on exposure to continuous illumination^{42, 47}. Initial investigations focused on bulk materials, but it was later observed and studied at the nanoscale, which became a reason for the effect to be described as a 'bulk' photovoltaic effect (BPVE); while the term 'anomalous' photovoltaic effect (APVE) was used due to experimental observations of photovoltages 10³ to 10⁴ times higher at open circuit in contrast to the band gap of the material^{42, 46}. Not all ferroelectrics exhibit an APVE, as it is dependent on the polarization magnitude¹²⁸, direction of polarization^{41, 48, 129}, light intensity¹³⁰, electrode spacing^{131, 132}, electrical conductivity⁴⁶ and the crystallography of the material^{131, 133, 134}, in addition to the nature of domain walls^{40, 41} and material/electrode interfaces¹¹⁵. Its dependence on so many factors often leads to difficulty in reproducing the APVE, even in the same material 112, 113. Therefore, several models have been proposed to explain the distinct type and nature of photoferroic effects. These include Schottky-junction effects, depolarization field effects and interface and domain wall effects^{40, 41}, which are now described below.

4.1. Bulk Photovoltaic Effect (BPVE)

The first model of BPVE was proposed by Glass et. al.¹³⁵ which was based on the asymmetry in materials. In recent years, Rappe and co-workers have developed theories based on shift currents¹³⁶⁻¹⁴⁰. Consequently, BPVE and APVE could now be explained at the microscopic level using *ballistic* and *shift* mechanism models^{47, 49}. The *ballistic model* for isotropic and anisotrpic materials in centrosymmetric (in the general case for p-n junction solar cells) and noncentrosymmetric crystals (in the general case for ferroelectric solar cells and asymmetric hybrid perovskite solar cells) is explained using Figure 7 (a) and (b), respectively⁵⁰. This manifests itself in that on exposure to an appropriate illumination the thermalized/hot carrier from the valence band excites to the conduction band, thereby leading to the generation of a photocurrent. However, the presence of asymmetry or non-centrosymmetry in crystals leads to a disparity in a momentum distribution of the carriers in the conduction band. The carrier then loses its energy and settles at the bottom of the conduction band by undergoing a band-band transition or a shift by distance l_0 so as to equilibrate the asymmetric momentum and hence generating an additional photocurrent leading to BPVE^{49, 50}.

< Figure 7>

Figure 7: (a) Isotropic and (b) anisotropic non-equilibrium carriers' momentum distribution in centrosymmetric (general case for p-n junction solar cells) and non-centrosymmetric (general case for ferroelectric solar cells and asymmetric hybrid perovskite solar cells) corresponding to the classical and bulk photovoltaic effects, respectively. Adapted from references^{47,50}

In contrast, the *shift current* mechanism has a quantum-mechanical nature and the behavior of the thermalized carriers is governed by coherent excitations, rather than inelastic scattering, which allows for the net current flow from the asymmetry of the potential^{136, 140, 141}. The same mechanism is also supported by experimentally verified first principle studies on BaTiO₃ and PbTiO₃ ferroelectrics^{136, 137}, multiferroic BiFeO₃ ¹³⁷and hybrid halide perovskites CH₃NH₃PbI₃ and CH₃NH₃PbI₃-xClx ¹³⁸. It is also suggested that the material itself can act as a current source^{97,101,104} and the effect is also dependent on electronic structure and bonding interactions¹³⁶. The total photocurrent (J) of a ferroelectric material in the closed circuit condition can be given as the sum of steady current density (J_{sc}) generated due to illumination and the contribution of dark- (σ_{cl}) and photo- (σ_{cbh}) conductivities:

$$J = J_{sc} + (\sigma_d + \sigma_{ph})E \quad \text{or} \quad J = J_{sc} + (\sigma_d + \sigma_{ph})\frac{V}{d}$$
 (2)

where E is the internal electric field developed between electrodes separated by distance d, and V is the applied voltage. In the open circuit condition, the total current (J) will vanish and hence the open circuit voltage (V_{oc}) is given as:

$$V_{oc} = \frac{J_{sc}d}{(\sigma_d + \sigma_{ph})} \tag{3}$$

The above expression suggests that V_{oc} will be anomalous if illumination leads to a significant rise in steady current density (J_{sc}). In addition, it is to be noted that the photoconductivity (σ_{ph}) is also dependent on light intensity^{49, 51, 135, 142-144}. If the rise in σ_{ph} during illumination is of the order of the rise in J_{sc} , then it will cancel out the influence of a rise in J_{sc} and cause the material to exhibit a constant or linear photoferroic effect. However, if there is a condition where $J_{sc} >> \sigma_{ph} >> \sigma_d$ then the effect will be 'anomalous' since V_{oc} in this case will increase abruptly. In

addition, if $\sigma_{ph}+\sigma_d$ is insensitive to the light intensity, or the change in σ_{ph} is small in comparison to the magnitude of σ_d , then this condition will also contribute towards the BPVE/APVE. In general, for most of the ferroelectric materials the case of $J_{sc}>>\sigma_{ph}>>\sigma_d$ exists and hence the V_{oc} for BPVE can be simplified to $\sim J_{sc}/\sigma_{ph}$. This can be further explained by substituting the following (μ : mobility of non-equilibrium charge carrier; α : absorption coefficient; τ : life time of non-equilibrium charge carrier; ξ : measure of exciton; l_0 : mean free path; asymmetry; hv: photon energy; φ : quantum yield; q: positive elementary charge; Δn : excess charge carrier concentration; ϕ_0 : photon flux density)^{50, 145}:

$$J_{sc} = q l_0 \xi \varphi \alpha \tag{4}$$

$$\sigma_{ph} = q(\mu_n + \mu_{ph}) \Delta n = q(\mu_n + \mu_{ph}) \varphi \alpha \tau \phi_0 \tag{5}$$

Hence, the efficiency of the BPVE/APVE can be calculated by using equation 1 and expressed as^{50, 145}:

$$\eta = \frac{J_{sc}^2}{\alpha I \sigma_{ph}} = \frac{J_{sc}^2}{\alpha I_0(\mu \tau)_{ph}} \quad \text{or} = \frac{q \alpha \phi (l_0 \xi)^2 d}{4(\mu_n + \mu_p) \tau h \nu} \text{ with an assumed FF of 25\%}$$
 (6)

Interestingly, the BPVE/APVE was first explained in ferroelectrics using the aforementioned models. However, the first evidence of the BPVE/APVE effect was reported in paraelectric BaTiO₃¹²³, non-ferroelectric cadmium telluride¹²⁴⁻¹²⁶ and zinc sulfide thin films¹²⁷. It was suggested that this is due to the formation of surface space-charge layers¹²³ or stacking faults that produced a cumulative internal depolarization field¹²⁷. Simultaneously, the same reasons were also thought to affect the process of domain nucleation¹²³.

4.2. Depolarization Field Driven Ferroelectric Photovoltaic Effect

Ferroelectric materials possess a spontaneous polarization, i.e. electric dipoles are formed inside the material. Ideally, if the ferroelectric is sandwiched between electrodes with the same workfunction then the built-in voltage due to the presence of dipoles must be balanced by the presence of charges at the electrodes. However, in practice the free charges at the electrodes are not able to completely cancel the space and polarization charges which gives rise to internal fields in the opposite direction of polarization¹⁴⁶. The cumulative internal field developed by these unscreened charges accumulated at the ferroelectric-metal interface is known as a depolarization field 145, 147. It has been shown that the depolarization field is capable of changing the overall magnitude of the polarization, transition temperature, coercive field and the order of the phase transitions ^{148, 149}. Interestingly, the polarization filed is dependent on the material as well as electrode thickness and the area of contact 148, 149.; it is negligible for a large inter-electrode distance in bulk ferroelectrics but is likely to increase with a reduction in inter-electrode distance, as in thin films^{131, 146, 148, 149}. This eventually makes it a governing factor for the photoferroelectric effect in thin films as they significantly influence both the screening of spontaneous polarization and the separation of the photo-generated charge carriers^{121, 150-152}. In this context, Pintilie and Alexe postulated that the polarization bound charge is not located at the electrode but is slightly away at an atomic distance δ from the electrode and hence results in the formation of surface dipole layers that lead to a modification in the surface injection barriers ¹⁵³. Furthermore. this built-in voltage (V_{bi}) due to the difference in work function of the electrodes is modified by the surface dipole layers and is given as 145:

$$V'_{bi} = V_{bi} + \frac{P_s \delta}{\varepsilon_0 \varepsilon_r} \tag{7}$$

The depolarization field for a metal contact with different dielectric constants (ε_{e1} and ε_{e2}) and screening lengths (l_{s1} and l_{s2}) for a dielectric constant (ε_F) can be written as ^{154, 155}:

$$F_{dp} = \frac{P}{\varepsilon_0 \varepsilon_F} \frac{\left(\frac{l_{s1}}{\varepsilon_{e1}} + \frac{l_{s2}}{\varepsilon_{e2}}\right)}{\left(\frac{l_{s1}}{\varepsilon_{e1}} + \frac{l_{s2}}{\varepsilon_{e2}}\right) + d}$$
(8)

The impact of the depolarization field on photovoltaic performance of thin films has been verified in several reports and it is believed that ultra-high thin films (films with thickness of a few nanometers) with high dielectric constant electrodes can aid in achieving high photovoltaic efficiencies ^{130, 131, 133, 146, 148-152, 156-158}. Furthermore, it has been illustrated that it is possible to control the transportation characteristics by controlling the direction of polarization¹⁵⁹. The control over transportation characteristics is also related to the Schottky barrier, which is another important mechanism for ferroelectric photovoltaics and will be discussed in the next section.

4.3. Ferroelectric Schottky-Junction Effect

A Schottky barrier is formed at a ferroelectric-metal electrode interface due to the difference in work-functions, which leads to the development of a local electric field. On illumination, this built-in field drives the photocurrents by band bending at the interface¹⁶⁰. Therefore, the barrier height and the depth of the depletion region plays an important role in the generation of photovoltages¹⁶⁰; which is by the constraints of the material band-gap and work-function of the electrode ^{113, 145, 147}. Due to this reason the effect is probably less well studied in contrast to the bulk photovoltaic effect (BPVE). The overall barrier height can be enhanced by sandwiching a ferroelectric semiconductor between electrodes of different materials with large difference in work function^{115, 159, 161-168}. This was first demonstrated by Blom *et. al.* in 1994¹⁶⁹ who sandwiched a ferroelectric PbTiO₃ film between a Schottky contact (Au) and an Ohmic bottom electrode (La_{0.5}Sr_{0.5}CoO₃) and showed that the Schottky barrier can be reduced by switching the

polarization in the direction of the ferroelectric polarization. Another popular mechanism of tuning the barrier height and the width of depletion region is to tune charged defects^{163, 170}. In this context, the most common defect, namely oxygen vacancies, have been studied in hybrid halide perovskites^{171, 172} and ferroelectrics^{115, 170}. However, the photovoltaic effect obtained using this mechanism is not very stable as the poled state of oxygen vacancies usually becomes unstable on removal of the electric field over time. However, it remains very useful in distinguishing between the depolarization and Schottky junction based photovoltaic mechanism as it is possible to have switchable diode-like rectifying behavior using the Schottky junction effect is independent of the direction of polarization field¹¹⁵. Interestingly, the Schottky junction effect is independent of the direction of polarization and, therefore, it can be used to distinguish it from BPVE¹⁷³. The understanding developed to date can aid in tuning the Schottky junction effect to support BPVE and achieve a combined photovoltaic response.

4.4. Interface and Domain Wall Effects

Domain walls in complex oxides have been the focus of intense research over recent years. The fact that domain walls can be electrically conducting opens new pathways for a number of possible applications. Provided in the possible applications are possible applications. Recently anomalous photovoltaic effects related to domain walls in ferroelectric materials have been reported. Interestingly, electric-field control over domain structure allows the photovoltaic effect to be reversed in polarity or even to be turned off in such materials. The band structure and local bandgap of domain walls in ferroelectrics have also been studied. In addition, photo-induced electrochemical effects at domain walls are a further interesting route in applications in water splitting or for domain wall decoration (see 190 and references therein).

The spatial and temporal evolution of photoinduced charge generation and carrier separation in heteroepitaxial BiFeO₃ thin films was measured with Kelvin probe and piezoresponse force microscopy. Polycopy. Contributions from the self-poled and ferroelectric polarization charge were identified from the time evolution of the correlated surface potential and ferroelectric polarization in both, films as-grown and after poling, and at different stages and intensities of optical illumination. Variations in the surface potential with bias voltage, switching history, and illumination intensity were investigated. It was shown that both bulk ferroelectric photovoltaic and the domain wall offset potential mechanisms contribute to the photogenerated charge. Polycrystalline 150, 2-D interfaces, 192-195 and 1-D ferroelectric nanostructures have also been explored for enhanced photovoltaic responses 196, 197, in addition to nanoscale enhancements of ferroelectric photovoltaic effects at metal nano-tips. 116

4.5 An Overview of Ferroelectric Photovoltaic Materials

Table 1 provides an insight into the photo-ferroelectric response of selected ferroelectric materials and their corresponding mechanism. In addition to these attempts and a history of over 40 years of study, there remains much to be learned before a ferroelectric photovoltaic device reaches any niche applications market. Although it is understood that non-centrosymmetry and polarization plays a crucial role in the bulk and depolarization field driven photovoltaic effect, the dynamics of the process remains unclear. The understanding of how exactly ferroelectricity helps in achieving an enhanced photo-response is an open question ¹⁶⁸. Moreover, from the photovoltaics view-point, there is a strong requirement of developing new ferroelectrics with a narrow bandgap and improved conductivity. Thereafter, domain wall engineering and a controlled polarization can aid in raising the photovoltaic efficiency to new levels. In addition,

there is a need to systematically understand charge carrier dynamics, such as mobility and diffusion length. Beyond this, other important considerations are the presence of piezo- and pyro-electricity in ferroelectrics. The photovoltaic response of ferroelectrics could be tuned under stress or hydrostatic pressure. Recently, Wang *et. al.* made an analogous attempt on hybrid perovskites and realized that it is possible to tune both the structural and optical properties by applying a pressure on the material¹⁹⁸. However, this needs special arrangement, but the pyroelectric effect could be exploited in parallel to photovoltaic effect to enhance the overall energy conversion.

5. Pyroelectric Effect

The effect of generating an electric charge due to changes in remnant and/or saturation polarization as a result of thermal fluctuations is known as the *pyroelectric effect*^{31, 37, 199, 200}. Figure 8 shows the schematic of time dependent thermal fluctuations that lead to a displacement of the central ion in a non-centrosymmetric perovskite and results in a change in output voltage. This can be used to supply an electrical current by using a resistive load. The change in polarization (ΔP_i) with temperature change (ΔT) is given as²⁰¹:

$$\Delta P_i = p\Delta T \tag{9}$$

where, p is the pyroelectric coefficient perpendicular to direction of the electrodes (i.e. in the polarization direction). Further, for a given surface area A, the induced short circuit current (I_P) for a given rate of temperature change (dT/dt) is 201,202

$$I_{P} = Ap \frac{dT}{dt} \tag{10}$$

In order to characterize enhanced pyroelectric energy conversion various figures of merit (FOMs) have been developed for the selection of appropriate pyroelectric materials depending on the thermal system and electrical circuits employed²⁰². The first pyroelectric FOMs were based on the maximum current or voltage for applications related to thermal detectors²⁰³⁻²⁰⁵.

< Figure 8>

Figure 8: Schematic presentation of pyroelectric effect where time dependent thermal fluctuations cause the displacement of the central atom in a non-centrosymmetric perovskite and results in an output voltage.

To achieve a high voltage responsivity (F_v) , the figure of merit²⁰³ to maximize the voltage for a given thermal input is given by Eqn. 11,

$$F_i = \frac{p}{c_E} = \frac{p}{\rho \cdot c_p} \tag{12}$$

In the case of a pyroelectric detector dominated by Johnson noise, the detector figure of merit is²⁰²,

$$F_D = \frac{p}{c_E \sqrt{\varepsilon_{33}^{\sigma} tan\delta}} \tag{13}$$

Eqns. 11 to 13 are FOMs that have been used to select materials for thermal detection, however for energy-harvesting the generated power is a criterion, along with the efficiency of the conversion of thermal energy to electrical energy. For energy harvesting applications, pyroelectric FOMs have been proposed^{36, 206} and an electro-thermal coupling factor estimates the effectiveness of thermal harvesting³⁶:

$$k^2 = \frac{p^2 \cdot T_{hot}}{c_E \cdot \varepsilon_{33}^{\sigma}} = \frac{p^2 \cdot T_{hot}}{\rho \cdot c_p \cdot \varepsilon_{33}^{\sigma}}$$
(14)

where T_{hot} is the maximum working temperature. An energy-harvesting FOM, F_E , has also been proposed²⁰⁶:

$$F_E = \frac{p^2}{\varepsilon_{33}^{\sigma}} \tag{15}$$

Eqn. 15 has been used for materials selection and materials design^{29, 207-210} for pyroelectric harvesting applications. Compared to the voltage (F_v) and current (F_i) responsivities, F_E does not consider the material heat capacity. Therefore, a modified pyroelectric thermal harvesting figure of merit, F'_E , has been derived when the harvesting device is subjected to an incident heat source of specific energy density ²¹¹⁻²¹³, which is given by:

$$F_E' = \frac{p^2}{\varepsilon_{33}^{\sigma} \cdot (c_E)^2} \tag{16}$$

Eqn. 16 indicates that good materials should have a high pyroelectric coefficient to develop a large charge with a temperate change, a low permittivity to develop a large potential difference because of the charge generated and a low volume specific heat to ensure the temperature rise due to the incident power density is large. It may be of interest to also consider losses and develop a figure of merit which includes loss, such as the $\tan \delta$ used in F_D (Eqn. 13).

In addition to the figures of merit for pyroelectric energy conversion, it has been suggested that the short circuit current can be enhanced to several orders of magnitude by employing thermal energy conversion cycles. In this context, Mohammadi and Khodayari advocated for the use of an Ericsson cycle ²¹⁴ knowing that there exist several other cycles based on the mode of operation^{36, 39}. These include resistive cycles³⁶, synchronized electric charge

extraction cycles^{36, 39} and synchronized switch damping on inductor (SSDI) cycles. Details about these cycles can be found in reference²². It has been found that the *Olsen cycle*, a well-known variant of the Ericson cycle, stands out in this regime²¹⁵⁻²¹⁷.

5.1. Olsen Cycle

The Olsen cycle operates under unipolar electric fields, rather than bipolar electric fields used in the conventional Ericson cycle, and therefore has a reduced hysteresis loss and enhanced energy conversion. The energy harvested using the Olsen cycle is not merely a contribution of the pyroelectric effect but also takes advantage of the electrical energy storage capacity of the material as a result of the change in capacitance (permittivity) with temperature. For this reason, the cycle is claimed to be capable of providing an energy density of three orders in magnitude higher than that obtained using the conventional pyroelectric effect ²³. Olsen et. al. experimentally verified this claim for a number of well-known compositions²¹⁵⁻²²² which has been supported by a number of studies ^{13-17, 23-25, 27, 209, 223}. This made the Olsen cycle the primary mechanism for pyroelectric energy harvesting. Since the cycle is based on temperature dependent polarization behavior, it is important to note that, in general, the saturation polarization decreases with an increase in temperature and such a response is referred to as a 'thermal fluctuations-1 (TF-1)' behavior while the case where the saturation polarization increases with an increase in temperature, i.e. where the hysteresis loop tends to become linear at low temperatures rather than at high temperatures, is known as 'thermal fluctuations-2 (TF-2)' behavior^{17, 20}. Since TF-2 compositions were rarely observed before 2008, the Olsen cycle was initially proposed for the commonly observed TF-1 ferroelectrics. In 2014, Vats et. al. proposed a modified version of the Olsen cycle for TF-2 compositions ¹⁷ and generalized it for materials

that exhibit a change in polarization with temperature fluctuations^{17, 20}. Figure 9 (a) and (b) show the working principle of an Olsen cycle for TF-1 and TF-2 composition, respectively.

< Figure 9>

Figure 9: Working of an Olsen cycle for (a) TF-1 and (b) TF-2 compositions and the area covered by the loop 1-2-3-4 shows the harvested energy.

The modified cycle states that the material should initially be polarized under a unipolar applied electric field at the lower temperature (T_L) and then exposed to a heat source isoelectrically (E_H) . This leads to a polarization change (a decrease for TF-1 and increase for TF-2) that can be simultaneously converted into an electrical output. Subsequently, the material is depolarized under a unipolar applied electric field at a constant higher temperature (T_H) followed by an isoelectric (E_L) cooling step. This again provides an output electrical impulse in the form of harvested electrical energy. Figure 10 (a) and (b) provide a schematic explanation of a typical Olsen cycle for TF-1 and TF-2 materials, respectively. Further, the area enclosed (1-2-3-4) by the complete cycle on a corresponding P-E curve gives the net harvested output electrical energy density (N_D) per liter per unit cycle 24,221 :

$$N_D = \oint E.dP \tag{17}$$

Table 2 summaries the performance of selected compositions for pyroelectric energy conversion. It is important to note that for a material to work with a practical Olsen cycle, an arrangement is needed to achieve specialized oscillating heat currents and an external load circuit is required for receiving an electrical output. A variation in the design of such an arrangement can significantly influence the degree of harvested electrical energy density. It is important to note that pyroelectric energy conversion is based on a time dependent thermal fluctuation. At the same

time, there exists a mechanism which utilizes a thermal gradient to harvest electrical energy, as discussed in the next section.

6. Perovskites for Thermoelectrics

6.1. Ferroelectric-Thermoelectrics

Thermoelectric generators are devices which convert temperature differences into electrical energy. The principal phenomenon which underpins this energy conversion are the Seebeck effect (i.e. the conversion of a thermal gradient into electricity) and Peltier effect (i.e. achieving a temperature gradient by passing a current through two junctions). $^{224-226}$ The thermoelectric effect have been widely employed for scavenging of waste thermal energy and the efficiency of a material for thermoelectric application is measured by its figure of merit, zT: 52

$$zT = S^2 \sigma T / \kappa \tag{18}$$

Where, S is the Seebeck coefficient and is defined as the ratio of the voltage change induced by a temperature change for a material with thermal and electrical conductivities κ and σ respectively. $S^2\sigma$ is termed the thermoelectric power factor. To achieve a high thermoelectric efficiency the material should have high electronic charge carrier concentration ($\Box 10^{18}$ to $\Box 10^{21}$ cm⁻³) and high electronic conductivity. An increase in carrier concentration will not only increase the electric conductivity but simultaneously enhance thermal conductivity which results in a decrease of the zT value and reduced thermoelectric performance of the material. Apart from this, the major roadblocks in the development of materials for this technology include a limited working temperature range, the use of toxic chemicals and high processing costs, while some materials

such as chalcogenides and antimonides have issues of oxidation at high temperatures.⁵² In the search of potential candidate materials which can overcome the above mentioned issues, oxygendeficient ferroelectrics with high conductivities have provided a new direction.^{227, 228} SrTiO₃ based materials have been well studied but their zT values are limited to 0.1 due to moderate thermal conductivities.²²⁹⁻²³⁶ In addition, CaMnO₃-based systems have a high Seebeck coefficient, low thermal conductivity and tunable resistivity^{237, 238}, which are ideal properties for improved thermoelectric applications. Theoretical estimations suggests that it is possible to have zT values greater than one in CaMnO₃. ²³⁹ Lee et. al. reviewed future directions in ferroelectric based thermoelectricity and stressed the potential of obtaining a high thermoelectric effect in ntype perovskite $BaTiO_3$ and tungsten bronze $(Sr_{1-x}Ba_x)Nb_2O_{6-\delta}$ systems⁵² and concluded that improved thermoelectric performance of ferroelectrics could be achieved by a better understanding of the mechanism behind the electronic interactions, defect states and oxygen vacancies. However, from a device perspective it is easy to optimize a pyroelectric (as it is easy to have time dependent temperature change rather than inducing a large thermal gradient over a ferroelectric thin film or pellet) based system instead of a thermal gradient (thermoelectric effect) based system on ferroelectric materials.³³ Consequently, a maximum Carnot efficiency of merely 1.7% was reported using the thermoelectric effect, while the same is found to be 50% for a pyroelectric device.³³

6.2. Hybrid Halide Perovskites for Thermoelectrics

In parallel research efforts on ferroelectric thermoelectrics, there exists a branch of organic thermoelectric materials which have recently gained significant interest among researchers because of their relatively low cost of manufacture, ease of fabrication and possibility of developing flexible thermoelectric modules²⁴⁰. He and Galli conducted a pioneering first principle study of CH₃NH₃AI₃ (A=Pb and Sn) for thermoelectric applications and realized that it is possible to have a zT in the rage of 1 to 2 by engineering hybrid halide perovskite superlattices.⁵³ Their study suggests that these perovskites may possess a large carrier mobility due to small carrier effective masses and weak carrier-phonon interaction. These materials have a large Seebeck coefficient and low thermal conductivities which makes them ideal candidates for thermoelectric energy harvesting. However, their electrical conductivity needs to be enhanced and this could be done by chemical or photoinduced doping.²⁴¹ Lee et. al. have used Density Functional Theory to suggested that CH₃NH₃AI₃ has a poor thermoelectric performance but it can be increased to the levels of the existing best thermoelectric counterparts (Bi₂Te₃) by electron-doping.²⁴² The claim was further supported in a theoretical study by Filippetti et. al. where they reported the possibilities of achieving a room temperature thermoelectric effect with zT values ranging between 1 to 3.243 Thereafter, Wang and Lin conducted Molecular Dynamics simulations and provided atomistic insights on ultralow phonon transport over a wide temperature range in these materials.²⁴⁴ Recently, Zhao et. al. conducted a first principle study and suggested that hole-doping optimization could provide better thermoelectric performance over the electron-doped one.²⁴⁵ In addition, they proposed to tailor the organic cation vacancies for better thermoelectric performance. By taking advantage of tuning the electrical conductivity by optimized doping, these studies postulate that hybrid halide perovskite more suitable for thermoelectric energy conversion in contrast to their ferroelectric counterparts. However, at this stage it is difficult to accurately predict the exact status of these materials as thermoelectric generators due to the lack of experimental confirmation.

7. Perovskites for Energy Storage

7.1. Ferroelectric Perovskites for Capacitor Applications

Ferroelectric materials and their composites have been studied in detail for ultra-high density capacitor applications²⁴⁶⁻²⁵². When an electric field is applied to a ferroelectric material sandwiched between two electrodes, it is polarized and energy is stored. The maximum energy stored (U) in such a capacitor is given by²⁵³:

$$U = \frac{1}{2} \frac{CV^2}{Volume} = \frac{1}{2} \frac{\varepsilon \varepsilon_0 A}{t} \frac{(E_b t)^2}{Volume} = \frac{1}{2} \frac{\varepsilon \varepsilon_0 A}{t} \frac{(E_b t)^2}{tA} = \frac{1}{2} \varepsilon \varepsilon_0 E_b^2$$
 (19)

where, C is the capacitance and E_b is the dielectric breakdown strength of the intervening dielectric layer of thickness t and electrode contact area A. Eq 19 suggests that the energy stored in a ferroelectric capacitor is dependent on the dielectric constant (ε) and breakdown strength of the material. Therefore, research has focused on improving both parameters. In this context, ferroelectric-polymer and ferroelectric-glass composites are being explored and have been proven to be good alternatives $^{248-250}$. In addition, the energy stored can also be estimated from the polarization versus electric field behavior of the materials, as illustrated by the shaded area of Figure 10. This clearly indicates that for high energy storage, the material should have a low remnant polarization and high saturation polarization with a low hysteresis, as observed in the case of relaxor ferroelectrics in Figure 10 (b). It is to be noted that in addition to these parameters the material should also possess low leakage current and dielectric losses. 248 , $^{250-252}$ A more detailed discussion of the state-of-the-art progress can be found in a recent review by Liu *et al.* 246 Although ferroelectrics have a proven potential as a dielectric material in a parallel plate capacitor structure, hybrid halide perovskites cannot be used for the same application because of

their relatively high electronic conductivity and loss. However, they are suitable for an electrode material or an electrolyte in supercapacitors. ²⁵⁴⁻²⁵⁶

< Figure 10>

Figure 10: A schematic of energy density storage estimation (highlighted shaded area) from the Polarization–Electric field (*P-E*) behavior of (a) ferroelectric, (b) relaxor ferroelectric and (c) antiferroelectric materials. Adapted from references^{246, 251, 253}

7.2. Hybrid Halide Perovskites for Supercapacitors

Recently, Zhou reported a thin film electrochemical capacitor based on an organo-lead-triiodide perovskite which exhibited a stable capacitance beyond 10⁴ cycles²⁵⁶. Such an approach provides a novel dimension for studying the ionic properties of hybrid halide perovskites and developing new devices. Shortly after, a perspective article by Snaith *et al.* postulated that the high surface area and ionic mobility of hybrid halide perovskites could make it a good alternative as an electrode or electrolyte in a supercapacitor. ^{254, 255} The major difference between a supercapacitor and a parallel plate capacitor is that the dielectric layer is replaced by an electrolyte in-between the electrodes. The ions in the electrolyte respond to the electric field, in contrast to the dipoles in a dielectric. Although research in this area has only just begun (in 2016) the presence of ferroelectric domain walls and diploes could enhance the performance of these capacitors. The same reasons could also be helpful in utilizing these materials in battery applications, which will now be described.

7.3. Hybrid Halide Perovskites for Batteries

In 2015, Xia et. al reported that MAPbX₃ (X=Br, I) is a potential anode material for lithium ion batteries with a storage capacity of ~330 mAh g⁻¹.257 However, it is still not clear if the Li-ion was stored by intercalation or if it was a surface phenomenon. Moreover, rapid deterioration of the electrode was also a major obstruction in commercializing these materials in a battery. Further investigations in this direction revealed that post-poling ion migration is much faster at grain boundaries than within the grains²⁵⁸, which supports the claim of the Xia et. al.²⁵⁷ and has motivated researchers to develop novel perovskites to address the key challenges of achieving improved storage capacity and electrode stability at comparatively low cost, as compared to current commercially available batteries. Generally, solid state batteries are comprised of two lithium storing electrodes and an ion-conducting electrolyte. During charging, the lithium ions are driven into the anode by intercalation and the positive charge is compensated by the electrode.²⁵⁹ During discharge, the Li-ions move back to the cathode and the current produced by the corresponding reverse flow of electrons is used to power the device. To make this technology viable, critical milestone must be attained, which include fast ion migration with stable capacity and long cycling life.

8. Materials Selection and Future Prospects

The above discussion suggests that each technology and mechanism has its own desired characteristics, efficiency limit and corresponding advantages and disadvantages, such as a high band gap and low absorption coefficient restricts the photovoltaic performance in ferroelectrics, while technological constraints restrict single junction and silicon photovoltaics to 30% (Shockley and Queisser limit)²⁶⁰. Similarly, the ability to achieve a high thermoelectric operating temperature for ferroelectrics is an issue, while the absence of the desired electrical conductivity

in hybrid perovskites is an additional barrier for thermoelectric applications. Consequently, there is a need to develop new materials with a suitable range of properties for effective utilization of available solar and thermal resources. In parallel, the approach of simultaneously engaging multiple energy conversion mechanisms could be envisaged^{19, 261, 262}. One such illustration is reported by Zhang et.al. 160 who enlarged the photovoltaic response of a device by combining the classical photovoltaic effect with the ferroelectric photovoltaic effect; this was achieved by sandwiching lanthanum-modified lead zirconate titanate between two low work function metal electrodes. Using a similar concept, Zhu et. al. took advantage of a piezo-phototronic effect by using a ZnO nanowire array on a silicon substrate to achieve enhanced efficiency²⁶³. Other examples include the fabrication of a multi-functional nano-generator using PbZr_xTi_{1-x}O₃ that was integrated with an air-driven nylon membrane and thermoelectric module²⁶⁴, and the hybridization of electrical nano-generators and solar cells with supercapacitors for self-powered wearable electronic textiles²⁶⁵. Park et. al. demonstrated a hybrid energy conversion system with integrated pyroelectric and thermoelectric modules to harvest solar energy across the full spectral range and demonstrated switching of electrochromic displays using the approach. In an analogous approach, Kim et. al. demonstrated enhanced energy collection by integrating a photothermal, pyroelectric and thermoelectric module with a solar cell. ²⁶⁶ A detailed state-of-theart summary of nano-generator technologies based on mechanical (piezoelectric²⁶⁷ and triboelectric²⁶⁸), thermal (pyroelectric²⁶⁹ and thermoelectric²⁷⁰) and solar energy harvesting, their coupled mechanisms to harvest energy from multiple sources²⁷¹⁻²⁷⁵ and the possibilities of integrating energy harvesting devices with storage units^{276, 277} can be found in the literature^{261,} ²⁶². However, these systems require distinct materials and, therefore, a more complex device structure is required, compared to a device operating on a single material, which is likely to

increase losses. In contrast, a single material with an optimal combination of desired characteristics could enhance research effort in this direction.

To some extent most of the material property requirements for each application overlap with one another. Therefore, materials with overlapping desired properties for different applications could be used for a multiple energy conversion system. This will not only aid engineers and physicists in selecting an appropriate material from the existing pool of materials, but also provide insight for chemists and materials scientists for developing new materials. This could be achieved by employing appropriate materials selection techniques ²⁷⁸⁻²⁸⁴ or a detailed understanding of the individual material requirements which are discussed in the following subsections. Similar approaches be used to tune materials for a multiple energy conversion system.

8.1. Material Requirements for Hybrid Perovskite Solar Cells

Initially, a suitable material for photovoltaic applications must have good light absorption, carrier generation, carrier lifetime and mobility ²⁸⁵⁻²⁸⁷. The material should have a high absorption coefficient, which governs the generation of free carriers or excitons subjected to the binding energy, temperature and carrier density²⁸⁷. A perovskite layer should have modest mobility²⁸⁸ and a sufficiently high diffusion length which is a measurement of carrier transportation to the electrode before recombination²⁸⁵. In order to build efficient devices it is essential to optimize the film thickness and develop deposition and film treatment techniques for reliably producing good quality films²⁸⁷. It has been suggested that an appropriate selection of cations could facilitate spontaneous electrical polarization in these materials²⁸⁹. This will result in the creation of internal junctions at ferroelectric domains and help in the separation of photo-excited charge carriers. Therefore, an improved knowledge of the fundamental ferroelectric nature of potential

materials could significantly help in designing smart materials with better performance²⁹⁰. In addition, the presence of ferroelectric domains could aid the reduction of segregation assisted recombination of charge carriers²⁸⁵. The transportation could be adversely affected by the presence of defects, which is often increased by doping since it enhances carrier scattering and thus influences conductivity, minority carrier lifetime and mobility. Doping not only affects electrical transport, but also governs the operating mechanism of the device²⁸⁷. The attractive photovoltaic performance of hybrid halide perovskites is often attributed to a low density of trap defects ^{288, 291-293} or relatively shallow traps²⁹⁴⁻²⁹⁶. In addition, interface engineering that includes the development of alternate electron and hole transport materials or the use of doping can further improve the interface (morphologically and electrically) for charge transport²⁸⁵. Since the charge transport capability of a material also governs its suitability for supercapacitor and battery applications, any improvement to achieve better transport dynamics will also increase the suitability of these materials for supercapacitor and battery applications.

8.2. Material Requirements for Ferroelectric Photovoltaics

As with the hybrid halide perovskites, the photovoltaic performance of ferroelectrics is also governed by light absorption, generation and separation of excitons, and the transportation dynamics of the charge carriers. Unlike the hybrid halide perovskites, ferroelectrics typically have a high band gap and low absorption coefficients. In this context, several attempts have been made to reduce their band gap and to enhance absorption using doping^{297, 298}, alloying¹⁸⁷ and oxygen vacancies^{163, 299-301}. Though the presence of oxygen vacancies will enhance the conductivity of the ferroelectric and aid in charge transportation but a significant increase in conductivity will also lead to diminished ferroelectric polarization and enhanced leakage

currents. Therefore, it is important to develop a trade-off between conductivity and polarization. In addition, the internal photoelectric effect can be used to enhance light absorption 160. Although the absorption coefficient of ferroelectrics is typically low, their charge dissociation efficiency, due to a low binding energy, is high in contrast to hybrid halide perovskites. In general, ferroelectrics possess a high dielectric constant; which is inversely proportional to the binding energy of the excitons. However, the BPVE in ferroelectrics is governed by the noncentrosymmetric potential which is further dependent on the direction of polarization^{302, 303}. The pre-decay shift in excited charge carriers is merely a few angstrom in the direction of polarization which results in small photocurrents. 46 Therefore, it becomes important to increase the non-centrosymmetry in ferroelectrics. 136, 196, 304, 305 The idea of enhancing the photocurrent by increasing the non-centrosymmetry is also supported by experiments. 306-308 For the final stage of charge collection, a reduction in the ferroelectric film thickness is beneficial, but the photovoltages are decreased. 132 Another method for increasing the collecting charge electric field is by forming an extending depletion using metal/intrinsic semiconductor/metal structures.³⁰⁹ This could also be achieved by replacing the metal electrode with semiconductors which increases the depolarization field and charge collection efficiency by lowering the screening of spontaneous polarization. 121, 150 The depolarization field is strongly dependent on the screening conditions at the interface and the film thickness. 131, 146, 148, 149 Therefore, interface engineering and film thickness optimization are essential for high photovoltaic responses of ferroelectrics.

8.3. Material Requirements for Thermo-electrical energy conversion and Storage

The energy conversion using pyroelectric and thermoelectric effects could be termed as thermoelectrical energy conversion. For high pyroelectric energy conversion, the material should

have a high pyroelectric coefficient to have a large change in polarization with respect to temperature fluctuation $(\partial P/\partial T)$. Consequently, dielectric anomalies, phase transitions or instantaneous switching, creation/destruction of crystal domains and the Curie temperature should lie within the operating temperature range. In addition, the materials should possess a high breakdown strength and high dielectric constant to have a large change in polarization with a variation in applied electric field. Importantly, it should exhibit low losses and leakage currents 18, 223, 310 311. Interestingly, the requirements for high pyroelectric energy conversion are similar to the requirements for high energy storage in ferroelectric capacitors¹⁶. As far as the requirements for thermoelectric energy conversions are concerned, ferroelectrics lie far behind the hybrid halide perovskites. However, to date no experimental study has confirmed the thermoelectric performance of the hybrid halide perovskites. Only theoretical calculations have been performed and suggestions have been made to tune the electrical conductivity. However, one report claims that using a CaMnO₃ ferroelectric buffer layer with a hybrid halide perovskite could help in increasing the open circuit voltage and provide a better thermoelectric output.³¹² Similar attempts could help in creation of efficient energy conversion devices and makes it interesting to compile the materials requirements for possible multiple energy conversion devices.

9. Analogy in Material Requirements and Conclusions

There are theoretical reports where the pyroelectric effect is found to support the photovoltaic performance of the material. Recently, the possibility of tuning piezoelectric properties simply by illumination has been illustrated. The pyroelectric and dielectric properties simply by illumination has been illustrated. Moreover, it is also possible to take advantage of piezoelectricity to enhance pyroelectric pyroelectric.

solar cell performance¹⁹ and the performance of self-powered photodetectors³¹⁹. Interestingly, the ideal material requirements for photovoltaics are the same as for supercapacitor and battery applications. The same requirements with a tuned electrical conductivity also makes a hybrid halide perovskite suitable for thermoelectric applications. In this context, the efforts of doping and creating an understanding of the effect of oxygen vacancies could be adopted from ferroelectrics. Importantly, ideal properties for pyroelectric energy conversion and ferroelectric capacitors supplement photovoltaic effects in both ferroelectrics and perovskites. A stable hybrid organic-inorganic flexible ferroelectric material with a low band gap, high absorption coefficient and better charge transportation dynamics could become an excellent material for photovoltaic, supercapacitor and battery applications while a similar material with low thermal conductivity will be beneficial for thermoelectric effects. For pyroelectric energy conversion and ferroelectric capacitors, the leakage currents should be low and the existing properties with a high band gap, break-down strength and dielectric constant with low conductivity in a hybrid organic-inorganic material could provide a better conversion efficiency and storage. Such perovskite materials with improved storage and conversion efficiencies could be integrated together for better utilization of available thermal and solar resource. Clearly, if multiple energy conversion mechanisms are anticipated there is a need to develop synergies in the multifunctional properties of these materials. In summary, the information compiled herewith is aimed at motivating researchers to realize the potential of existing perovskites and to develop novel hybrid halide ferroelectric perovskites for multiple energy conversion and storage systems.

Acknowledgements

Richa acknowledge support from the Center of Excellence in Nanoelectronics (CEN), IIT Bombay, India. Gaurav, Jae, Anita and Jan acknowledge support by the Australian Government via the Australian Research Council (ARC) through Discovery Grants and the Australian Renewable Energy Agency.

References

- 1. P. IEA-PVPS, *Report IEA-PVPS T1-24*, 2014.
- 2. S. Chu, Y. Cui and N. Liu, *Nature Materials*, 2017, **16**, 16-22.
- 3. P. IEA-PVPS, Report IEA-PVPS 2010, 2010.
- 4. N.-G. Park, M. Grätzel, T. Miyasaka, K. Zhu and K. Emery, *Nature Energy*, 2016, **1**, 16152.
- 5. J. S. Manser, J. A. Christians and P. V. Kamat, *Chemical Reviews*, 2016, **116**, 12956-13008.
- 6. B. E. Hardin, H. J. Snaith and M. D. McGehee, *Nature Photonics*, 2012, **6**, 162-169.
- 7. H. J. Snaith, *The Journal of Physical Chemistry Letters*, 2013, **4**, 3623-3630.
- 8. M. A. Green, A. Ho-Baillie and H. J. Snaith, *Nature Photonics*, 2014, **8**, 506-514.
- 9. F. Giustino and H. J. Snaith, ACS Energy Letters, 2016.
- 10. N. A. Benedek and C. J. Fennie, *The Journal of Physical Chemistry C*, 2013, **117**, 13339-13349.
- 11. J. Young, P. Lalkiya and J. M. Rondinelli, Journal of Materials Chemistry C, 2016, 4, 4016-4027.
- 12. W. Rehman, D. P. McMeekin, J. B. Patel, R. L. Milot, M. B. Johnston, H. J. Snaith and L. M. Herz, *Energy & Environmental Science*, 2017.
- 13. A. Chauhan, S. Patel, G. Vats and R. Vaish, Energy Technology, 2014, 2, 205-209.
- 14. R. Sao, G. Vats and R. Vaish, Ferroelectrics, 2015, **474**, 1-7.
- 15. G. Vats, A. Chauhan and R. Vaish, *International Journal of Applied Ceramic Technology*, 2015, **12**, E49-E54.
- 16. G. Vats, H. S. Kushwaha and R. Vaish, *Materials Research Express*, 2014, 1, 015503.
- 17. G. Vats, R. Vaish and C. R. Bowen, Journal of Applied Physics, 2014, 115, 013505.
- 18. G. Vats, S. Patel, A. Chauhan and R. Vaish, *International Journal of Applied Ceramic Technology*, 2015, **12**, 765-770.
- 19. G. Vats, S. Patel and R. Vaish, *Integrated Ferroelectrics*, 2016, **168**, 69-84.
- 20. G. Vats, A. Kumar, N. Ortega, C. R. Bowen and R. S. Katiyar, *Energy & Environmental Science*, 2016, **9**, 1335-1345.
- 21. C. Bowen, H. Kim, P. Weaver and S. Dunn, Energy & Environmental Science, 2014.
- 22. C. Bowen, J. Taylor, E. LeBoulbar, D. Zabek, A. Chauhan and R. Vaish, *Energy & Environmental Science*, 2014.
- 23. R. Kandilian, A. Navid and L. Pilon, Smart Materials and Structures, 2011, 20, 055020.
- 24. F. Y. Lee, S. Goljahi, I. M. McKinley, C. S. Lynch and L. Pilon, *Smart Materials and Structures*, 2012, **21**, 025021.
- 25. F. Y. Lee, A. Navid and L. Pilon, Applied Thermal Engineering, 2012, 37, 30-37.
- 26. I. M. McKinley, S. Goljahi, C. S. Lynch and L. Pilon, *Journal of Applied Physics*, 2013, **114**, 224111.
- 27. I. M. McKinley, R. Kandilian and L. Pilon, Smart Materials and Structures, 2012, 21, 035015.
- 28. I. M. McKinley, F. Y. Lee and L. Pilon, *Applied energy*, 2014, **126**, 78-89.
- 29. A. Navid and L. Pilon, *Smart Materials and Structures*, 2011, **20**, 025012.
- 30. A. Navid, D. Vanderpool, A. Bah and L. Pilon, *International Journal of Heat And Mass Transfer*, 2010, **53**, 4060-4070.

- 31. D. Guyomar, S. Pruvost and G. Sebald, *Ultrasonics, Ferroelectrics and Frequency Control, IEEE Transactions on*, 2008, **55**, 279-285.
- 32. D. Guyomar, G. Sebald, E. Lefeuvre and A. Khodayari, *Journal of Intelligent Material Systems and Structures*, 2009, **20**, 265-271.
- 33. G. Sebald, D. Guyomar and A. Agbossou, Smart Materials and Structures, 2009, 18, 125006.
- 34. G. Sebald, E. Lefeuvre and D. Guyomar, *Ultrasonics, Ferroelectrics and Frequency Control, IEEE Transactions on*, 2008, **55**, 538-551.
- 35. G. Sebald, S. Pruvost and D. Guyomar, Smart Materials and Structures, 2008, 17, 015012.
- 36. G. Sebald, E. Lefeuvre and D. Guyomar, *IEEE Transactions on Ultrasonics, Ferroelectrics, and Frequency Control*, 2008, **55**.
- 37. A. Khodayari, S. Pruvost, G. Sebald, D. Guyomar and S. Mohammadi, *Ultrasonics, Ferroelectrics and Frequency Control, IEEE Transactions on*, 2009, **56**, 693-699.
- 38. H. Zhu, S. Pruvost, D. Guyomar and A. Khodayari, *Journal of Applied Physics*, 2009, **106**, 124102.
- 39. D. Guyomar and M. Lallart, 2009.
- 40. J. Seidel, D. Fu, S.-Y. Yang, E. Alarcón-Lladó, J. Wu, R. Ramesh and J. W. Ager III, *Physical Review Letters*, 2011, **107**, 126805.
- 41. S. Yang, J. Seidel, S. Byrnes, P. Shafer, C.-H. Yang, M. Rossell, P. Yu, Y.-H. Chu, J. Scott and J. Ager, *Nature Nanotechnology*, 2010, **5**, 143-147.
- 42. V. M. Fridkin and B. Popov, Soviet Physics Uspekhi, 1978, 21, 981.
- 43. V. Fridkin, A. Grekov, P. Ionov, A. Rodin, E. Savchenko and K. Mikhailina, *Ferroelectrics*, 1974, **8**, 433-435.
- 44. V. Fridkin, *Applied Physics*, 1977, **13**, 357-359.
- 45. L. BELYAEV, V. Fridkin, A. Grekov, N. Kosonogov and A. Rodin, *Le Journal de Physique Colloques*, 1972, **33**, C2-123-C122-125.
- 46. V. M. Fridkin, *Photoferroelectrics*, Springer Science & Business Media, 2012.
- 47. J. E. Spanier, V. M. Fridkin, A. M. Rappe, A. R. Akbashev, A. Polemi, Y. Qi, Z. Gu, S. M. Young, C. J. Hawley and D. Imbrenda, *Nature Photonics*, 2016.
- 48. V. Fridkin, *Crystallography Reports*, 2001, **46**, 654-658.
- 49. B. I. Sturman and V. M. Fridkin, *Photovoltaic and Photo-refractive Effects in Noncentrosymmetric Materials*, Gordon and Breach Publishers, 1992.
- 50. A. Zenkevich, Y. Matveyev, K. Maksimova, R. Gaynutdinov, A. Tolstikhina and V. Fridkin, *Physical Review B*, 2014, **90**, 161409.
- 51. A. Grekov, M. MA, V. Spitsyna and V. Fridkin, *SOVIET PHYSICS CRYSTALLOGRAPHY, USSR*, 1970, **15**, 423-&.
- 52. S. Lee, J. A. Bock, S. Trolier-McKinstry and C. A. Randall, *Journal of the European Ceramic Society*, 2012, **32**, 3971-3988.
- 53. Y. He and G. Galli, *Chemistry of Materials*, 2014, **26**, 5394-5400.
- 54. International Technology Roadmap for Photovoltaic (ITRPV) 2015.
- 55. M. A. Green, *Solar cells: operating principles, technology, and system applications,* Englewood Cliffs, NJ, Prentice-Hall, Inc., 1982. 288 p., 1982.
- 56. A. Fahrenbruch and R. Bube, *Fundamentals of solar cells: photovoltaic solar energy conversion,* Elsevier, 2012.
- 57. B. A. Gregg, *The Journal of Physical Chemistry B*, 2003, **107**, 4688-4698.
- 58. S. Pfuetzner, J. Meiss, A. Petrich, M. Riede and K. Leo, Applied Physics Letters, 2009, 94, 3307.
- 59. B. O'regan and M. Grätzel, *Nature*, 1991, **353**, 737-740.
- 60. S. Ardo and G. J. Meyer, *Chemical Society Reviews*, 2009, **38**, 115-164.
- 61. A. Hagfeldt, G. Boschloo, L. Sun, L. Kloo and H. Pettersson, *Chemical Reviews*, 2010, **110**, 6595-6663.

- 62. U. Bach, D. Lupo, P. Comte, J. Moser, F. Weissörtel, J. Salbeck, H. Spreitzer and M. Grätzel, *Nature*, 1998, **395**, 583-585.
- 63. K. Murakoshi, R. Kogure, Y. Wada and S. Yanagida, *Chemistry Letters*, 1997, 471-472.
- 64. N. Robertson, *Angewandte Chemie International Edition*, 2006, **45**, 2338-2345.
- 65. A. Mishra, M. K. Fischer and P. Bäuerle, *Angewandte Chemie International Edition*, 2009, **48**, 2474-2499.
- 66. S. Huang, G. Schlichthörl, A. Nozik, M. Grätzel and A. Frank, *The Journal of Physical Chemistry B*, 1997, **101**, 2576-2582.
- 67. G. Boschloo and A. Hagfeldt, Accounts of Chemical Research, 2009, 42, 1819-1826.
- 68. J. Bisquert, F. Fabregat-Santiago, I. Mora-Sero, G. Garcia-Belmonte and S. Giménez, *The Journal of Physical Chemistry C*, 2009, **113**, 17278-17290.
- 69. Y. Chiba, A. Islam, Y. Watanabe, R. Komiya, N. Koide and L. Han, *Japanese Journal of Applied Physics*, 2006, **45**, L638.
- 70. F. Gao, Y. Wang, D. Shi, J. Zhang, M. Wang, X. Jing, R. Humphry-Baker, P. Wang, S. M. Zakeeruddin and M. Grätzel, *Journal of the American Chemical Society*, 2008, **130**, 10720-10728.
- 71. C.-Y. Chen, M. Wang, J.-Y. Li, N. Pootrakulchote, L. Alibabaei, C.-h. Ngoc-le, J.-D. Decoppet, J.-H. Tsai, C. Grätzel and C.-G. Wu, *ACS Nano*, 2009, **3**, 3103-3109.
- 72. M. A. Green and A. W.-Y. Ho-Baillie, ACS Energy Letters, 2017.
- 73. D. Mitzi, S. Wang, C. Feild, C. Chess and A. Guloy, *Science*, 1995, **267**, 1473.
- 74. D. B. Mitzi, K. Chondroudis and C. R. Kagan, *IBM Journal of Research and Development*, 2001, **45**, 29-45.
- 75. A. Kojima, K. Teshima, T. Miyasaka and Y. Shirai, 2006.
- 76. A. Kojima, K. Teshima, Y. Shirai and T. Miyasaka, *Journal of the American Chemical Society*, 2009, **131**, 6050-6051.
- 77. A. Kojima, K. Teshima, Y. Shirai and T. Miyasaka, 2008.
- 78. J.-H. Im, C.-R. Lee, J.-W. Lee, S.-W. Park and N.-G. Park, *Nanoscale*, 2011, **3**, 4088-4093.
- 79. H.-S. Kim, C.-R. Lee, J.-H. Im, K.-B. Lee, T. Moehl, A. Marchioro, S.-J. Moon, R. Humphry-Baker, J.-H. Yum and J. E. Moser, *Scientific Reports*, 2012, **2**, 591.
- 80. M. M. Lee, J. Teuscher, T. Miyasaka, T. N. Murakami and H. J. Snaith, *Science*, 2012, **338**, 643-647.
- 81. S. D. Stranks, G. E. Eperon, G. Grancini, C. Menelaou, M. J. Alcocer, T. Leijtens, L. M. Herz, A. Petrozza and H. J. Snaith, *Science*, 2013, **342**, 341-344.
- 82. J. H. Heo, S. H. Im, J. H. Noh, T. N. Mandal, C.-S. Lim, J. A. Chang, Y. H. Lee, H.-j. Kim, A. Sarkar and M. K. Nazeeruddin, *Nature Photonics*, 2013, **7**, 486-491.
- 83. J. H. Noh, S. H. Im, J. H. Heo, T. N. Mandal and S. I. Seok, *Nano Letters*, 2013, **13**, 1764-1769.
- 84. J. Burschka, N. Pellet, S.-J. Moon, R. Humphry-Baker, P. Gao, M. K. Nazeeruddin and M. Grätzel, *Nature*, 2013, **499**, 316-319.
- 85. M. Liu, M. B. Johnston and H. J. Snaith, *Nature*, 2013, **501**, 395-398.
- 86. N. J. Jeon, J. H. Noh, Y. C. Kim, W. S. Yang, S. Ryu and S. I. Seok, *Nature Materials*, 2014, **13**, 897-903.
- 87. N. J. Jeon, J. H. Noh, W. S. Yang, Y. C. Kim, S. Ryu, J. Seo and S. I. Seok, *Nature*, 2015, **517**, 476-480.
- 88. R. Service, *Science*, 2014, **344**, 458.
- 89. H. Zhou, Q. Chen, G. Li, S. Luo, T.-b. Song, H.-S. Duan, Z. Hong, J. You, Y. Liu and Y. Yang, *Science*, 2014, **345**, 542-546.
- W. S. Yang, J. H. Noh, N. J. Jeon, Y. C. Kim, S. Ryu, J. Seo and S. I. Seok, *Science*, 2015, 348, 1234-1237.
- 91. M. A. Green, *Progress in Photovoltaics: Research and Applications*, 2017, **25**, 333-334.

- 92. K. A. Bush, A. F. Palmstrom, J. Y. Zhengshan, M. Boccard, R. Cheacharoen, J. P. Mailoa, D. P. McMeekin, R. L. Hoye, C. D. Bailie and T. Leijtens, *Nature Energy*, 2017, **2**, 17009.
- 93. C. Lévy-Clément, R. Tena-Zaera, M. A. Ryan, A. Katty and G. Hodes, *Advanced Materials*, 2005, **17**, 1512-1515.
- 94. Y. Itzhaik, O. Niitsoo, M. Page and G. Hodes, *The Journal of Physical Chemistry C*, 2009, **113**, 4254-4256.
- 95. G. E. Eperon, V. M. Burlakov, P. Docampo, A. Goriely and H. J. Snaith, *Advanced Functional Materials*, 2014, **24**, 151-157.
- 96. J. M. Ball, M. M. Lee, A. Hey and H. J. Snaith, *Energy & Environmental Science*, 2013, **6**, 1739-1743.
- 97. M. A. Green and S. P. Bremner, *Nature Materials*, 2017, **16**, 23-34.
- 98. F. Hao, C. C. Stoumpos, D. H. Cao, R. P. Chang and M. G. Kanatzidis, *Nature Photonics*, 2014, **8**, 489-494.
- 99. S. Wang, Y. Jiang, E. J. Juarez-Perez, L. K. Ono and Y. Qi, *Nature Energy*, 2016, **2**, 16195.
- 100. S. S. Shin, E. J. Yeom, W. S. Yang, S. Hur, M. G. Kim, J. Im, J. Seo, J. H. Noh and S. I. Seok, *Science*, 2017, **356**, 167-171.
- 101. B. Chen, J. Shi, X. Zheng, Y. Zhou, K. Zhu and S. Priya, *Journal of Materials Chemistry A*, 2015, **3**, 7699-7705.
- 102. Z. Sun, X. Liu, T. Khan, C. Ji, M. A. Asghar, S. Zhao, L. Li, M. Hong and J. Luo, *Angewandte Chemie*, 2016, **128**, 6655-6660.
- 103. P.-F. Li, Y.-Y. Tang, Z.-X. Wang, H.-Y. Ye, Y.-M. You and R.-G. Xiong, *Nature Communications*, 2016, **7**, 13635.
- 104. H.-W. Chen, N. Sakai, M. Ikegami and T. Miyasaka, *The Journal of Physical Chemistry Letters*, 2014, **6**, 164-169.
- 105. Z. Fan, J. Xiao, K. Sun, L. Chen, Y. Hu, J. Ouyang, K. P. Ong, K. Zeng and J. Wang, *The Journal Of Physical Chemistry Letters*, 2015, **6**, 1155-1161.
- 106. J. M. Frost, K. T. Butler and A. Walsh, *APL Materials*, 2014, **2**, 081506.
- 107. G. A. Sewvandi, K. Kodera, H. Ma, S. Nakanishi and Q. Feng, Scientific Reports, 2016, 6.
- 108. S. N. Rashkeev, F. El-Mellouhi, S. Kais and F. H. Alharbi, Scientific Reports, 2015, 5.
- 109. D.-F. Pan, G.-F. Bi, G.-Y. Chen, H. Zhang, J.-M. Liu, G.-H. Wang and J.-G. Wan, *Scientific Reports*, 2016, **6**.
- 110. P. S. Brody and F. Crowne, *Journal of Electronic Materials*, 1975, **4**, 955-971.
- 111. E. Krätzig and H. Kurz, Ferroelectrics, 1976, **13**, 295-296.
- 112. K. T. Butler, J. M. Frost and A. Walsh, Energy & Environmental Science, 2015, 8, 838-848.
- 113. Y. Yuan, Z. Xiao, B. Yang and J. Huang, Journal of Materials chemistry A, 2014, 2, 6027-6041.
- 114. Y. Jiang, X. Wen, A. Benda, R. Sheng, A. W. Ho-Baillie, S. Huang, F. Huang, Y.-B. Cheng and M. A. Green, *Solar Energy Materials and Solar Cells*, 2016, **151**, 102-112.
- 115. W. Ji, K. Yao and Y. C. Liang, *Advanced Materials*, 2010, **22**, 1763-1766.
- 116. M. Alexe and D. Hesse, *Nature Communications*, 2011, **2**, 256.
- 117. A. Bhatnagar, A. R. Chaudhuri, Y. H. Kim, D. Hesse and M. Alexe, *Nature Communications*, 2013, **4**.
- 118. I. Grinberg, D. V. West, M. Torres, G. Gou, D. M. Stein, L. Wu, G. Chen, E. M. Gallo, A. R. Akbashev and P. K. Davies, *Nature*, 2013, **503**, 509-512.
- 119. J. Kreisel, M. Alexe and P. A. Thomas, *Nature Materials*, 2012, **11**, 260-260.
- 120. D. Daranciang, M. J. Highland, H. Wen, S. M. Young, N. C. Brandt, H. Y. Hwang, M. Vattilana, M. Nicoul, F. Quirin and J. Goodfellow, *Physical Review Letters*, 2012, **108**, 087601.
- 121. M. Qin, K. Yao and Y. C. Liang, *Applied Physics Letters*, 2008, **93**, 122904.
- 122. A. M. Prokhorov, Ferroelectric crystals for laser radiation control, Taylor & Francis, 1990.

- 123. A. Chynoweth, *Physical Review*, 1956, **102**, 705.
- 124. L. Pensak, *Physical Review*, 1958, **109**, 601.
- 125. B. Goldstein and L. Pensak, Journal of Applied Physics, 1959, 30, 155-161.
- 126. B. Goldstein, *Physical Review*, 1958, **109**, 601.
- 127. S. Ellis, F. Herman, E. Loebner, W. Merz, C. Struck and J. White, *Physical Review*, 1958, **109**, 1860.
- 128. P. S. Brody, *Applied Physics Letters*, 1981, **38**, 153-155.
- 129. L. Pintilie, I. Vrejoiu, G. Le Rhun and M. Alexe, *Journal of Applied Physics*, 2007, **101**, 064109.
- 130. P. Brody, *Solid State Communications*, 1973, **12**, 673-676.
- 131. M. Qin, K. Yao, Y. C. Liang and S. Shannigrahi, Journal of Applied Physics, 2007, 101, 014104.
- 132. M. Ichiki, R. Maeda, Y. Morikawa, Y. Mabune, T. Nakada and K. Nonaka, *Applied Physics Letters*, 2004, **84**, 395-397.
- 133. M. Ichiki, H. Furue, T. Kobayashi, R. Maeda, Y. Morikawa, T. Nakada and K. Nonaka, *Applied Physics Letters*, 2005, **87**, 222903.
- 134. M. Ichiki, Y. Morikawa, Y. Mabune and T. Nakada, *Journal of the European Ceramic Society*, 2004, **24**, 1709-1714.
- 135. A. Glass, D. Von der Linde and T. Negran, *Applied Physics Letters*, 1974, **25**, 233-235.
- 136. S. M. Young and A. M. Rappe, *Physical Review Letters*, 2012, **109**, 116601.
- 137. S. M. Young, F. Zheng and A. M. Rappe, Physical Review Letters, 2012, 109, 236601.
- 138. F. Zheng, H. Takenaka, F. Wang, N. Z. Koocher and A. M. Rappe, *The Journal of Physical Chemistry Letters*, 2014, **6**, 31-37.
- 139. S. M. Young, F. Zheng and A. M. Rappe, *Physical Review Letters*, 2013, **110**, 057201.
- 140. L. Z. Tan, F. Zheng, S. M. Young, F. Wang, S. Liu and A. M. Rappe, *NPJ Computational Materials*, 2016, **2**, 16026.
- 141. R. von Baltz and W. Kraut, *Physical Review B*, 1981, **23**, 5590.
- 142. R. Guo, L. You, Y. Zhou, Z. S. Lim, X. Zou, L. Chen, R. Ramesh and J. Wang, *Nature Communications*, 2013, **4**.
- 143. P. Gunter, Ferroelectrics, 1978, **22**, 671-674.
- 144. Z. Wu, Y. Zhang, K. Ma, Y. Cao, H. Lin, Y. Jia, J. Chen and H. Li, *Physica Status Solidi (RRL)-Rapid Research Letters*, 2014, **8**, 36-39.
- 145. P. Lopez-Varo, L. Bertoluzzi, J. Bisquert, M. Alexe, M. Coll, J. Huang, J. A. Jimenez-Tejada, T. Kirchartz, R. Nechache and F. Rosei, *Physics Reports*, 2016, **653**, 1-40.
- 146. R. Mehta, B. Silverman and J. Jacobs, Journal of Applied Physics, 1973, 44, 3379-3385.
- 147. Z. Fan, K. Sun and J. Wang, *Journal of Materials Chemistry A*, 2015, **3**, 18809-18828.
- 148. I. Batra, P. Wurfel and B. Silverman, *Physical Review B*, 1973, **8**, 3257.
- 149. P. Wurfel and I. Batra, *Physical Review B*, 1973, **8**, 5126.
- 150. B. Chen, M. Li, Y. Liu, Z. Zuo, F. Zhuge, Q.-F. Zhan and R.-W. Li, *Nanotechnology*, 2011, **22**, 195201.
- 151. B. Chen, Z. Zuo, Y. Liu, Q.-F. Zhan, Y. Xie, H. Yang, G. Dai, Z. Li, G. Xu and R.-W. Li, *Applied Physics Letters*, 2012, **100**, 173903.
- 152. W. Dong, Y. Guo, B. Guo, H. Liu, H. Li and H. Liu, *Materials Letters*, 2013, **91**, 359-361.
- 153. L. Pintilie and M. Alexe, *Journal of Applied Physics*, 2005, **98**, 124103.
- 154. M. Y. Zhuravlev, R. F. Sabirianov, S. Jaswal and E. Y. Tsymbal, *Physical Review Letters*, 2005, **94**, 246802.
- 155. D. Pantel and M. Alexe, *Physical Review B*, 2010, **82**, 134105.
- 156. C. Ahn, K. Rabe and J.-M. Triscone, *Science*, 2004, **303**, 488-491.
- 157. M. Qin, K. Yao and Y. C. Liang, *Applied Physics Letters*, 2009, **95**, 022912.
- 158. M. Ichiki, Y. Morikawa and T. Nakada, *Japanese Journal of Applied Physics*, 2002, **41**, 6993.

- 159. D. Lee, S. Baek, T. Kim, J.-G. Yoon, C. Folkman, C. Eom and T. Noh, *Physical Review B*, 2011, **84**, 125305.
- 160. J. Zhang, X. Su, M. Shen, Z. Dai, L. Zhang, X. He, W. Cheng, M. Cao and G. Zou, *Scientific Reports*, 2013, **3**.
- 161. M. Qin, K. Yao and Y. C. Liang, *Journal of Applied Physics*, 2009, **105**, 061624.
- 162. M. Qin, K. Yao, Y. C. Liang and B. K. Gan, Applied Physics Letters, 2007, 91, 092904.
- 163. H. Yi, T. Choi, S. Choi, Y. S. Oh and S. W. Cheong, *Advanced Materials*, 2011, **23**, 3403-3407.
- 164. P. Zhang, D. Cao, C. Wang, M. Shen, X. Su, L. Fang, W. Dong and F. Zheng, *Materials Chemistry and Physics*, 2012, **135**, 304-308.
- 165. K. Yao, B. K. Gan, M. Chen and S. Shannigrahi, Applied Physics Letters, 2005, 87, 212906.
- 166. Z. Fan, W. Ji, T. Li, J. Xiao, P. Yang, K. P. Ong, K. Zeng, K. Yao and J. Wang, *Acta Materialia*, 2015, **88**, 83-90.
- 167. Y. Yang, S. Lee, S. Yi, B. Chae, S. Lee, H. Joo and M. Jang, *Applied Physics Letters*, 2000, **76**, 774-776.
- 168. L. Fang, L. You, Y. Zhou, P. Ren, Z. Shiuh Lim and J. Wang, *Applied Physics Letters*, 2014, **104**, 142903.
- 169. P. Blom, R. Wolf, J. Cillessen and M. Krijn, *Physical Review Letters*, 1994, **73**, 2107.
- 170. Y. Guo, B. Guo, W. Dong, H. Li and H. Liu, *Nanotechnology*, 2013, **24**, 275201.
- 171. Z. Xiao, Y. Yuan, Y. Shao, Q. Wang, Q. Dong, C. Bi, P. Sharma, A. Gruverman and J. Huang, *Nature Materials*, 2015, **14**, 193-198.
- 172. Y. Zhao, C. Liang, H. Zhang, D. Li, D. Tian, G. Li, X. Jing, W. Zhang, W. Xiao and Q. Liu, *Energy & Environmental Science*, 2015, **8**, 1256-1260.
- 173. F. Zheng, J. Xu, L. Fang, M. Shen and X. Wu, *Applied Physics Letters*, 2008, **93**, 172101.
- 174. J. Seidel, The Journal of Physical Chemistry Letters, 2012, **3**, 2905-2909.
- 175. H. Huang, *Nature Photonics*, 2010, **4**, 134-135.
- 176. J. Seidel, G. Singh-Bhalla, Q. He, S.-Y. Yang, Y.-H. Chu and R. Ramesh, *Phase Transitions*, 2013, **86**, 53-66.
- 177. Y. P. Chiu, Y. T. Chen, B. C. Huang, M. C. Shih, J. C. Yang, Q. He, C. W. Liang, J. Seidel, Y. C. Chen and R. Ramesh, *Advanced Materials*, 2011, **23**, 1530-1534.
- 178. J. Seidel, P. Maksymovych, Y. Batra, A. Katan, S.-Y. Yang, Q. He, A. P. Baddorf, S. V. Kalinin, C.-H. Yang and J.-C. Yang, *Physical Review Letters*, 2010, **105**, 197603.
- 179. J. Seidel, S.-Y. Yang, E. Alarcòn-Lladò, J. Ager III and R. Ramesh, *Ferroelectrics*, 2012, **433**, 123-126.
- 180. H. Matsuo, Y. Kitanaka, R. Inoue, Y. Noguchi, M. Miyayama, T. Kiguchi and T. J. Konno, *Physical Review B*, 2016, **94**, 214111.
- 181. C. Blouzon, J. Chauleau, A. Mougin, S. Fusil and M. Viret, *Physical Review B*, 2016, **94**, 094107.
- 182. R. Inoue, S. Ishikawa, R. Imura, Y. Kitanaka, T. Oguchi, Y. Noguchi and M. Miyayama, *Scientific Reports*, 2015, **5**.
- 183. H.-J. Feng, M. Wang, F. Liu, B. Duan, J. Tian and X. Guo, *Journal of Alloys and Compounds*, 2015, **628**, 311-316.
- 184. S. Liu, F. Zheng, N. Z. Koocher, H. Takenaka, F. Wang and A. M. Rappe, *The Journal of Physical Chemistry Letters*, 2015, **6**, 693-699.
- 185. A. Lubk, S. Gemming and N. Spaldin, *Physical Review B*, 2009, **80**, 104110.
- 186. O. Diéguez, P. Aguado-Puente, J. Junquera and J. Íñiguez, Physical Review B, 2013, 87, 024102.
- 187. W. S. Choi, M. F. Chisholm, D. J. Singh, T. Choi, G. E. Jellison Jr and H. N. Lee, *Nature Communications*, 2012, **3**, 689.
- 188. J. C. Wojdeł and J. Iniguez, *Physical Review Letters*, 2014, **112**, 247603.
- 189. A. Kudo and Y. Miseki, *Chemical Society Reviews*, 2009, **38**, 253-278.

- 190. A. Haussmann, P. Milde, C. Erler and L. M. Eng, *Nano Letters*, 2009, **9**, 763-768.
- 191. F. Yan, G. Chen, L. Lu and J. E. Spanier, ACS Nano, 2012, **6**, 2353-2360.
- 192. T. Choi, L. Jiang, S. Lee, T. Egami and H. N. Lee, New Journal of Physics, 2012, 14, 093056.
- 193. L. Pintilie, C. Dragoi and I. Pintilie, Journal of Applied Physics, 2011, 110, 044105.
- 194. T. Qu, Y. Zhao, D. Xie, J. Shi, Q. Chen and T. Ren, Applied Physics Letters, 2011, 98, 173507.
- 195. C. Tu, C. Hung, V. Schmidt, R. Chien, M. Jiang and J. Anthoninappen, *Journal of Physics: Condensed Matter*, 2012, **24**, 495902.
- 196. G. Gopal Khan, R. Das, N. Mukherjee and K. Mandal, *Physica Status Solidi (RRL)-Rapid Research Letters*, 2012, **6**, 312-314.
- 197. X. Zhang, H. Liu, B. Zheng, Y. Lin, D. Liu and C.-W. Nan, Journal of Nanomaterials, 2013, 2013, 3.
- 198. L. Wang, K. Wang and B. Zou, The Journal of Physical Chemistry Letters, 2016, 7, 2556-2562.
- 199. M. Ikura, Ferroelectrics, 2002, **267**, 403-408.
- 200. L. Kouchachvili and M. Ikura, *International Journal of Energy Research*, 2008, **32**, 328-335.
- 201. R. Whatmore, Ferroelectrics, 1991, 118, 241-259.
- 202. R. Whatmore, Reports on Progress In Physics, 1986, 49, 1335.
- 203. S. B. Lang and D. Das-Gupta, Handbook of Advanced Electronic and Photonic Materials and Devices, 2000, **4**, 22-50.
- 204. J. Cooper, Journal of Scientific Instruments, 1962, **39**, 467.
- 205. E. Putley, *Infrared Physics*, 1980, **20**, 139-147.
- 206. G. Sebald, L. Seveyrat, D. Guyomar, L. Lebrun, B. Guiffard and S. Pruvost, *Journal of Applied Physics*, 2006, **100**, 124112-124116.
- 207. R. Mangalam, J. Agar, A. Damodaran, J. Karthik and L. Martin, *ACS Applied Materials & Interfaces*, 2013, **5**, 13235-13241.
- 208. S. Ravindran, T. Huesgen, M. Kroener and P. Woias, Applied Physics Letters, 2011, 99, 104102.
- 209. A. Navid, C. S. Lynch and L. Pilon, *Smart Materials and Structures*, 2010, **19**, 055006.
- 210. S. Ravindran, T. Huesgen, M. Kroener and P. Woias, 2011.
- 211. S. H. Krishnan, D. Ezhilarasi, G. Uma and M. Umapathy, *IEEE transactions on sustainable energy*, 2014, **5**, 73-81.
- 212. A. Cuadras, M. Gasulla and V. Ferrari, Sensors and Actuators A: Physical, 2010, 158, 132-139.
- 213. C.-C. Hsiao and A.-S. Siao, *Sensors*, 2013, **13**, 12113-12131.
- 214. S. Mohammadi and A. Khodayari, Smart Materials Research, 2012, 2012.
- 215. R. Olsen and D. Bruno, 1986.
- 216. R. B. Olsen, D. A. Bruno and J. M. Briscoe, Journal of Applied Physics, 1985, **58**, 4709-4716.
- 217. R. B. Olsen, D. A. Bruno, J. M. Briscoe and E. W. Jacobs, *Journal of applied physics*, 1985, **57**, 5036-5042.
- 218. R. Olsen and D. Brown, *Ferroelectrics*, 1982, **40**, 17-27.
- 219. R. Olsen, D. Bruno, J. Briscoe and J. Dullea, Ferroelectrics, 1984, 59, 205-219.
- 220. R. B. Olsen, *Journal of Energy*, 1982, **6**, 91-95.
- 221. R. B. Olsen, J. M. Briscoe, D. A. Bruno and W. F. Butler, *Ferroelectrics*, 1981, **38**, 975-978.
- 222. R. B. Olsen and D. Evans, *Journal of applied physics*, 1983, **54**, 5941-5944.
- 223. G. Vats, H. S. Kushwaha, R. Vaish, N. A. Madhar, M. Shahabuddin, J. M. Parakkandy and K. M. Batoo, *Journal of Advanced Dielectrics*, 2014, **4**, 1450029.
- 224. H. Goldsmid, *Thermoelectric refrigeration*, Springer, 2013.
- 225. H. J. Goldsmid, 1960.
- 226. T. Tritt, Recent Trends in Thermoelectric Materials Research, Part Two, Academic Press, 2000.
- 227. S. Lee, R. H. Wilke, S. Trolier-McKinstry, S. Zhang and C. A. Randall, *Applied Physics Letters*, 2010, **96**, 031910.
- 228. S. Lee, S. Dursun, C. Duran and C. A. Randall, Journal of Materials Research, 2011, 26, 26-30.

- 229. T. Okuda, K. Nakanishi, S. Miyasaka and Y. Tokura, *Physical Review B*, 2001, **63**, 113104.
- 230. H. Frederikse, W. Thurber and W. Hosler, *Physical Review*, 1964, **134**, A442.
- 231. H. Ohta, *Materials Today*, 2007, **10**, 44-49.
- 232. B. Jalan and S. Stemmer, *Applied Physics Letters*, 2010, **97**, 042106.
- 233. C. Yu, M. L. Scullin, M. Huijben, R. Ramesh and A. Majumdar, *Applied Physics Letters*, 2008, **92**, 092118.
- 234. H. Muta, K. Kurosaki and S. Yamanaka, Journal of Alloys and Compounds, 2003, 350, 292-295.
- 235. M. L. Scullin, J. Ravichandran, C. Yu, M. Huijben, J. Seidel, A. Majumdar and R. Ramesh, *Acta Materialia*, 2010, **58**, 457-463.
- 236. M. L. Scullin, C. Yu, M. Huijben, S. Mukerjee, J. Seidel, Q. Zhan, J. Moore, A. Majumdar and R. Ramesh, *Applied Physics Letters*, 2008, **92**, 202113.
- 237. M. Ohtaki, H. Koga, T. Tokunaga, K. Eguchi and H. Arai, *Journal of Solid State Chemistry*, 1995, **120**, 105-111.
- 238. R. Kabir, T. Zhang, D. Wang, R. Donelson, R. Tian, T. T. Tan and S. Li, *Journal of Materials Science*, 2014, **49**, 7522-7528.
- 239. F. Zhang, Q. Lu, X. Zhang and J. Zhang, *Journal of Physics and Chemistry of Solids*, 2013, **74**, 1859-1864.
- 240. Y. Chen, Y. Zhao and Z. Liang, Energy & Environmental Science, 2015, 8, 401-422.
- 241. X. Mettan, R. Pisoni, P. Matus, A. Pisoni, J. i. Jaćimović, B. Náfrádi, M. Spina, D. Pavuna, L. Forró and E. Horváth, *The Journal of Physical Chemistry C*, 2015, **119**, 11506-11510.
- 242. C. Lee, J. Hong, A. Stroppa, M.-H. Whangbo and J. H. Shim, *RSC Advances*, 2015, **5**, 78701-78707.
- 243. A. Filippetti, C. Caddeo, P. D. Delugas and A. Mattoni, *The Journal of Physical Chemistry C*, 2016.
- 244. M. Wang and S. Lin, *Advanced Functional Materials*, 2016, **26**, 5297-5306.
- 245. T. Zhao, D. Wang and Z. Shuai, Synthetic Metals, 2017, 225, 108-114.
- 246. Z. Yao, Z. Song, H. Hao, Z. Yu, M. Cao, S. Zhang, M. T. Lanagan and H. Liu, *Advanced Materials*, 2017.
- 247. J. Scott, Science, 2007, **315**, 954-959.
- 248. P. Kim, N. M. Doss, J. P. Tillotson, P. J. Hotchkiss, M.-J. Pan, S. R. Marder, J. Li, J. P. Calame and J. W. Perry, *ACS Nano*, 2009, **3**, 2581-2592.
- 249. V. Tomer, G. Polizos, E. Manias and C. Randall, Journal of Applied Physics, 2010, 108, 074116.
- 250. V. Tomer, E. Manias and C. Randall, Journal of Applied Physics, 2011, 110, 044107.
- 251. I. Burn and D. Smyth, Journal of Materials Science, 1972, 7, 339-343.
- 252. G. R. Love, Journal of the American Ceramic Society, 1990, 73, 323-328.
- 253. N. Ortega, A. Kumar, J. Scott, D. B. Chrisey, M. Tomazawa, S. Kumari, D. Diestra and R. Katiyar, *Journal of Physics: Condensed Matter*, 2012, **24**, 445901.
- 254. W. Zhang, G. E. Eperon and H. J. Snaith, *Nature Energy*, 2016, **1**, 16048.
- 255. J. Beilsten-Edmands, G. Eperon, R. Johnson, H. Snaith and P. Radaelli, *Applied Physics Letters*, 2015, **106**, 173502.
- 256. S. Zhou, L. Li, H. Yu, J. Chen, C. P. Wong and N. Zhao, Advanced Electronic Materials, 2016, 2.
- 257. H.-R. Xia, W.-T. Sun and L.-M. Peng, Chemical Communications, 2015, **51**, 13787-13790.
- 258. Y. Shao, Y. Fang, T. Li, Q. Wang, Q. Dong, Y. Deng, Y. Yuan, H. Wei, M. Wang and A. Gruverman, *Energy & Environmental Science*, 2016, **9**, 1752-1759.
- 259. M. Winter and R. J. Brodd, Journal, 2004.
- 260. W. Shockley and H. J. Queisser, Journal of Applied Physics, 1961, 32, 510-519.
- 261. J.-H. Lee, J. Kim, T. Y. Kim, M. S. Al Hossain, S.-W. Kim and J. H. Kim, *Journal of Materials Chemistry A*, 2016, **4**, 7983-7999.
- 262. Z. L. Wang, G. Zhu, Y. Yang, S. Wang and C. Pan, *Materials Today*, 2012, **15**, 532-543.
- 263. L. Zhu, L. Wang, C. Pan, L. Chen, F. Xue, B. Chen, L. Yang, L. Su and Z. L. Wang, ACS Nano, 2017.

- 264. K. Zhang, S. Wang and Y. Yang, Advanced Energy Materials, 2016.
- 265. Z. Wen, M.-H. Yeh, H. Guo, J. Wang, Y. Zi, W. Xu, J. Deng, L. Zhu, X. Wang and C. Hu, *Science Advances*, 2016, **2**, e1600097.
- 266. E. Kim, T. Park, J. Na, B. Kim, Y. Kim and H. Shin, *Solar & Alternative Energy SPIE*, 2016, DOI: 10.1117/2.1201604.006377.
- 267. Z. L. Wang and J. Song, *Science*, 2006, **312**, 242-246.
- 268. F.-R. Fan, Z.-Q. Tian and Z. L. Wang, *Nano Energy*, 2012, **1**, 328-334.
- 269. Y. Yang, W. Guo, K. C. Pradel, G. Zhu, Y. Zhou, Y. Zhang, Y. Hu, L. Lin and Z. L. Wang, *Nano Letters*, 2012, **12**, 2833-2838.
- 270. B. Russ, A. Glaudell, J. J. Urban, M. L. Chabinyc and R. A. Segalman, *Nature Reviews Materials*, 2016, **1**, 16050.
- 271. Y. Zhang, J. Fang, C. He, H. Yan, Z. Wei and Y. Li, *The Journal of Physical Chemistry C*, 2013, **117**, 24685-24691.
- 272. J. H. Lee, K. Y. Lee, M. K. Gupta, T. Y. Kim, D. Y. Lee, J. Oh, C. Ryu, W. J. Yoo, C. Y. Kang and S. J. Yoon, *Advanced Materials*, 2014, **26**, 765-769.
- 273. Y. Zi, L. Lin, J. Wang, S. Wang, J. Chen, X. Fan, P. K. Yang, F. Yi and Z. L. Wang, *Advanced Materials*, 2015, **27**, 2340-2347.
- 274. Y. Yang, H. Zhang, G. Zhu, S. Lee, Z.-H. Lin and Z. L. Wang, *ACS Nano*, 2012, **7**, 785-790.
- 275. Y. Yang and Z. L. Wang, *Nano Energy*, 2015, **14**, 245-256.
- 276. X. Xue, S. Wang, W. Guo, Y. Zhang and Z. L. Wang, *Nano Letters*, 2012, **12**, 5048-5054.
- 277. H. Chang and Z.-R. Yu, *Journal of Nanoscience and Nanotechnology*, 2012, **12**, 6811-6816.
- 278. G. Vats, *Multi-Attribute Decision Making for Ferroelectric Materials Selection*, Lambert Academic Publishers, 2014.
- 279. G. Vats and R. Vaish, *Journal of Advanced Ceramics*, 2013, **2**, 141-148.
- 280. G. Vats and R. Vaish, Journal of Asian Ceramic Societies, 2014, 2, 5-10.
- 281. G. Vats and R. Vaish, *Advanced Science Focus*, 2014, **2**, 140-147.
- 282. G. Vats and R. Vaish, *International Journal of Applied Ceramic Technology*, 2014, **11**, 883-893.
- 283. G. Vats, R. Vaish and C. R. Bowen, *International Journal of Applied Ceramic Technology*, 2015, **12**, E1-E7.
- 284. G. Vats, M. Sharma, R. Vaish, V. S. Chauhan, N. A. Madhar, M. Shahabuddin, J. M. Parakkandy and K. M. Batoo, *Ferroelectrics*, 2015, **481**, 64-76.
- 285. P. Gao, M. Grätzel and M. K. Nazeeruddin, Energy & Environmental Science, 2014, 7, 2448-2463.
- 286. A. R. b. M. Yusoff and M. K. Nazeeruddin, *The Journal of Physical Chemistry Letters*, 2016, **7**, 851-866.
- 287. T. M. Brenner, D. A. Egger, L. Kronik, G. Hodes and D. Cahen, *Nature Reviews Materials*, 2016, **1**, 15007.
- 288. D. Shi, V. Adinolfi, R. Comin, M. Yuan, E. Alarousu, A. Buin, Y. Chen, S. Hoogland, A. Rothenberger and K. Katsiev, *Science*, 2015, **347**, 519-522.
- 289. J. M. Frost, K. T. Butler, F. Brivio, C. H. Hendon, M. Van Schilfgaarde and A. Walsh, *Nano Letters*, 2014, **14**, 2584-2590.
- 290. H. Röhm, T. Leonhard, M. J. Hoffmann and A. Colsmann, Energy & Environmental Science, 2017.
- 291. S. De Wolf, J. Holovsky, S.-J. Moon, P. Löper, B. Niesen, M. Ledinsky, F.-J. Haug, J.-H. Yum and C. Ballif, *The Journal of Physical Chemistry Letters*, 2014, **5**, 1035-1039.
- 292. K. Tvingstedt, O. Malinkiewicz, A. Baumann, C. Deibel, H. J. Snaith, V. Dyakonov and H. J. Bolink, *Scientific Reports*, 2014, **4**, 6071.
- 293. W. Tress, N. Marinova, O. Inganäs, M. Nazeeruddin, S. M. Zakeeruddin and M. Graetzel, *Advanced Energy Materials*, 2015, **5**.

- 294. H.-S. Duan, H. Zhou, Q. Chen, P. Sun, S. Luo, T.-B. Song, B. Bob and Y. Yang, *Physical Chemistry Chemical Physics*, 2015, **17**, 112-116.
- 295. M. Samiee, S. Konduri, B. Ganapathy, R. Kottokkaran, H. A. Abbas, A. Kitahara, P. Joshi, L. Zhang, M. Noack and V. Dalal, *Applied Physics Letters*, 2014, **105**, 153502.
- 296. A. Baumann, S. Väth, P. Rieder, M. C. Heiber, K. Tvingstedt and V. Dyakonov, *The Journal of Physical Chemistry Letters*, 2015, **6**, 2350-2354.
- 297. F. Lüdtke, N. Waasem, K. Buse and B. Sturman, Applied Physics B, 2011, 105, 35.
- 298. G. Chanussot, V. Fridkin, G. Godefroy and B. Jannot, Applied Physics Letters, 1977, 31, 3-4.
- 299. W. M. Lee, J. H. Sung, K. Chu, X. Moya, D. Lee, C. J. Kim, N. D. Mathur, S. W. Cheong, C. H. Yang and M. H. Jo, *Advanced Materials*, 2012, **24**.
- 300. A. Dhar and A. Mansingh, *Journal of Applied Physics*, 1990, **68**, 5804-5809.
- 301. L. Pintilie and I. Pintilie, *Materials Science and Engineering: B*, 2001, **80**, 388-391.
- 302. A. Glass, D. Von der Linde, D. Auston and T. Negran, *Journal of Electronic Materials*, 1975, **4**, 915-943.
- 303. C. W. Tang, Applied Physics Letters, 1986, 48, 183-185.
- 304. B. Kang, B. K. Rhee, G.-T. Joo, S. Lee and K.-S. Lim, Optics Communications, 2006, 266, 203-206.
- 305. J. W. Bennett and K. M. Rabe, Journal of Solid State Chemistry, 2012, 195, 21-31.
- 306. P. Poosanaas and K. Uchino, *Materials Chemistry and Physics*, 1999, **61**, 36-41.
- 307. A. Dogan, A. Prasadarao, K. Uchino, P. Poosanaas and S. Komarneni, *Journal of Electroceramics*, 1997, **1**, 105-111.
- 308. S. Shannigrahi and K. Yao, *Applied Physics Letters*, 2005, **86**, 092901.
- 309. Y. Zang, D. Xie, X. Wu, Y. Chen, Y. Lin, M. Li, H. Tian, X. Li, Z. Li and H. Zhu, *Applied Physics Letters*, 2011, **99**, 132904.
- 310. G. Vats, A. Kumar, N. Ortega, C. R. Bowen and R. S. Katiyar, *Energy & environmental science*, 2016, **9**, 2383-2391.
- 311. J. Scott, Annual Review of Materials Research, 2011, 41, 229-240.
- 312. P. Zhao, J. Xu, H. Wang, L. Wang, W. Kong, W. Ren, L. Bian and A. Chang, *Journal of Applied Physics*, 2014, **116**, 194901.
- 313. A. Katti and R. Yadav, *Physics Letters A*, 2017, **381**, 166-170.
- 314. Q. Jiang, Y. Su and X. Ji, *Physics Letters A*, 2012, **376**, 3085-3087.
- 315. V. G. Karpov and D. Shvydka, *Physica Status Solidi (RRL)-Rapid Research Letters*, 2007, **1**, 132-134.
- 316. M. Coll, A. s. Gomez, E. Mas-Marza, O. Almora, G. Garcia-Belmonte, M. Campoy-Quiles and J. Bisquert, *The Journal of Physical Chemistry Letters*, 2015, **6**, 1408-1413.
- 317. H. Borkar, V. Rao, S. Dutta, A. Barvat, P. Pal, M. Tomar, V. Gupta, J. Scott and A. Kumar, *Journal of Physics: Condensed Matter*, 2016, **28**, 265901.
- 318. H. Borkar, V. Rao, M. Tomar, V. Gupta, J. F. Scott and A. Kumar, *RSC Advances*, 2017, **7**, 12842-12855.
- 319. W. Peng, X. Wang, R. Yu, Y. Dai, H. Zou, A. C. Wang, Y. He and Z. L. Wang, *Advanced Materials*, 2017
- 320. R. Nechache, C. Harnagea, S. Licoccia, E. Traversa, A. Ruediger, A. Pignolet and F. Rosei, *Applied Physics Letters*, 2011, **98**, 202902.
- 321. V. Yarmarkin, B. Gol'tsman, M. Kazanin and V. Lemanov, *Physics of the Solid State*, 2000, **42**, 522-527.
- 322. T. Choi, S. Lee, Y. Choi, V. Kiryukhin and S.-W. Cheong, Science, 2009, 324, 63-66.
- 323. S. Yang, L. Martin, S. Byrnes, T. Conry, S. Basu, D. Paran, L. Reichertz, J. Ihlefeld, C. Adamo and A. Melville, *Applied Physics Letters*, 2009, **95**, 062909.
- 324. D. Cao, C. Wang, F. Zheng, W. Dong, L. Fang and M. Shen, *Nano Letters*, 2012, **12**, 2803-2809.

- 325. R. Katiyar, A. Kumar, G. Morell, J. Scott and R. Katiyar, *Applied Physics Letters*, 2011, **99**, 092906.
- 326. X. Hao, Y. Zhao and Q. Zhang, *The Journal of Physical Chemistry C*, 2015, **119** 18877–18885.
- 327. X. Hao, Y. Zhao and S. An, Journal of the American Ceramic Society, 2015, 98, 361-365.
- 328. M. H. Park, H. J. Kim, Y. J. Kim, T. Moon, K. Do Kim and C. S. Hwang, *Nano Energy*, 2015, **12**, 131-140.
- 329. M. H. Park, Y. H. Lee, H. J. Kim, Y. J. Kim, T. Moon, K. D. Kim, J. Müller, A. Kersch, U. Schroeder and T. Mikolajick, *Advanced Materials*, 2015, **27**, 1811-1831.

Table 1: Photovoltaic performance of ferroelectric materials.

Material	Fabricatio n Method	Photovoltage		Photo	current	Efficienc	Working	
		V _{oc} (V)	L (µm)	I _{sc} (μA cm ⁻²)	Light Intensity (mW cm ⁻²)	Light Wavelengt h (nm)	- y P _{out} /P _{in} (%)	Mechanism
Pt/PLZT(3/52 /48)/ITO ¹³²	MOD	0.86	4	1700	150	-	-	BPVE
		~496	2400	~16.8				
BaTiO ₃ ⁴⁷	Sputtering, FIB, PLD	8	-	17	100-470	405	100(EQE)	BPVE
Pt/Bi ₂ FECrO ₆ /Nb-SrTiO ₃ ³²⁰	PLD, Sputtering	0.74	0.125	990	1.5	635	6.5	BPVE
Au/PLWZT(3 /52/48)/Au ¹⁶⁵	Solution Coating	7.0	25	-	1.11	365	-	BPVE
ITO/PZT(53/4 7)/ITO ¹⁵¹	PLD	0.45	0.4	0.006	0.45	-	0.6	SCE & BPVE
Fe/BFO/LSM/ SrTiO ₃ ¹⁴²	PLD, Epitaxial	0.21	-	48	20	W-light	-	SCE & BPVE
Mg/PLZT(3/5 3/48)/ITO ¹⁶⁰	HPC	8.34	300	3.25	100	Sunlight	-	PE & BPVE
Pt:Pd/BFO/Pt :Pd ¹¹⁶	Mix-flux Technique	6 - 30	50- 300	10^{7} - 10^{8}	40,000	405	40(IQE)	TE & BPVE
Pt/PZT(20/80) /Pt ¹⁷³	Sputtering	-	0.36	~8	10	350-450	-	SCE & BPVE
Au/PLWZT(3 /52/48)/Au ¹⁶²	Sol-gel	0.6	0.706	-	0.74	365	-	SCE
Pt/PZT(52/48) /Pt or Ni ³²¹	Sol-gel	~0.8	0.2	~0.03	0.05	300-390	-	SCE

SrRuO ₃ /BFO/ ITO	MOCVD	0.8 - 0.9	0.2	1500	285	Sunlight	10 (EQE)	SCE
Au/BFO/Au ³²²	Mix-flux Technique	~0.08	80	8.219	<20	532	-	SCE
SrRuO ₃ /BFO/ Au ³²³	Sputtering, Epitaxial	0.286	0.17	0.4	750	435	-	SCE
Au/BFO/Au ¹⁶³	Mix-flux Technique	~0.7	60	1.58	20	532	1.5 (EQE)	SCE
Nb-doped SrTiO ₃ /BFO/ Au ¹⁹⁴	PLD	~0.15	0.1	6000	285	W-light	0.03	SCE
ITO/PZT/Cu ₂ O/Pt ³²⁴	Sol-gel	0.6	270	4800	100	Sunlight	0.57	SCE
Pt/Poly- BFO/Au & ITO ¹⁵⁰	Sol-gel	0.1	0.3	~1	450	340	-	SCE & DF
Graphene/Pol y-BFO/Pt ³⁰⁹	Sol-gel	0.20	0.3	2800	100	Sunlight	-	MIM-SCE
Nb: SrTiO ₃ /PLZT (3/52/48)/LSM	Sputtering, Epitaxial	~0.7	0.068	~0.8	0.059	-	0.28	DF
Pt/BFO/Pt ⁴¹	MOCVD	16	200	120	285	W-light	10 ⁻³ (EQE)	DW
Pt/BFO/Pt ⁴⁰	MOCVD	0.014	One DW	50	100	W-light	10(IQE)	DW
FTO/Poly- BFO/AZO ¹⁵²	CSD	0.63	-	130	100	Sunlight	7 (EQE)	BI & DF
ZnO: Al/BFO/LSC ³ 25	PLD	0.22	0.35	~5	1	W-light	-	-
Ag/Pr-doped BFO NTs/Ag ¹⁹⁶	Chemical Technique	0.21	-	-	10	Sunlight	~0.5	-

BPVE=bulk photovoltaic effect; DF=depolarization field effect; SCE=Schottky contact effect; DW=domain wall effect; MIM=metal/insulator/metal junction, PE=photoelectric effect;

BI=built-in potential due to asymmetric electrodes; TE=tip enhancement effect; MOD=metal—organic decomposition; MOVCD=metal—organic vapor phase epitaxial; FIB=Focused ion beam milling; PLD=pulsed laser deposition; HPC=hot-pressing calcinations; CSD=chemical solution deposition; IQE=internal quantum efficiency; EQE= external quantum efficiency

Table 2: Comparison of energy density and corresponding conditions for selected compositions.

Material	T _{Low}	T _{High} (K)	E _{Low}	E _{High}	Energy Density	
	(K)		(MVm ⁻¹)	(MVm^{-1})		
					(kJm ⁻³ cycle ⁻¹)	
73/27 P(VDF–TrFE) ^	296	340	23	53	30	
PZN-4.5PT ³⁷	373	433	0	2.0	217	
PZN-5.5PT ³⁵	373	463	0	1.2	150	
PMN-10PT ³⁵	303	353	0	3.5	186	
PMN-32PT ²³	353	443	0	0.9	100	
60/40 P(VDF–TrFE) ^	331	350	4.1	47.2	52	
PNZST ²¹⁶	418	448	0.8	3.2	300	
8/65/35 PLZT ^{#24}	298	433	0.2	7.5	888	
BNT-ST-BLT ¹⁴	293	413	0.1	6	2130	
KNTM ¹⁵	413	433	0.15	0.15	629	
BNLT ¹³	298	393	0.1	11.2	1146	
BNKT ¹³	298	383	0.1	5.2	1986	
BNK-BST ¹⁷	293	433	0.1	4.0	1523	
PLZST (x=0.2) #326	293	493	30	40	6800	
YBFO ^16	15	300	0.1	4	7570	
PLZST (x=0.18)# 327	298	573	30	90	7800	
0.67PMN-0.33PT ^223	303	323	0	60	6500	
0.68PMN-0.32PT ^223	303	323	0	60	8000	
$Hf_{0.2}Zr_{0.8}O_2^{328, 329}$	273	423	0	326	11549	

PZT/CFO/PZT^20	100	300	0	40	47372

^{*}Thick Films; ^Thin Films

Figures:

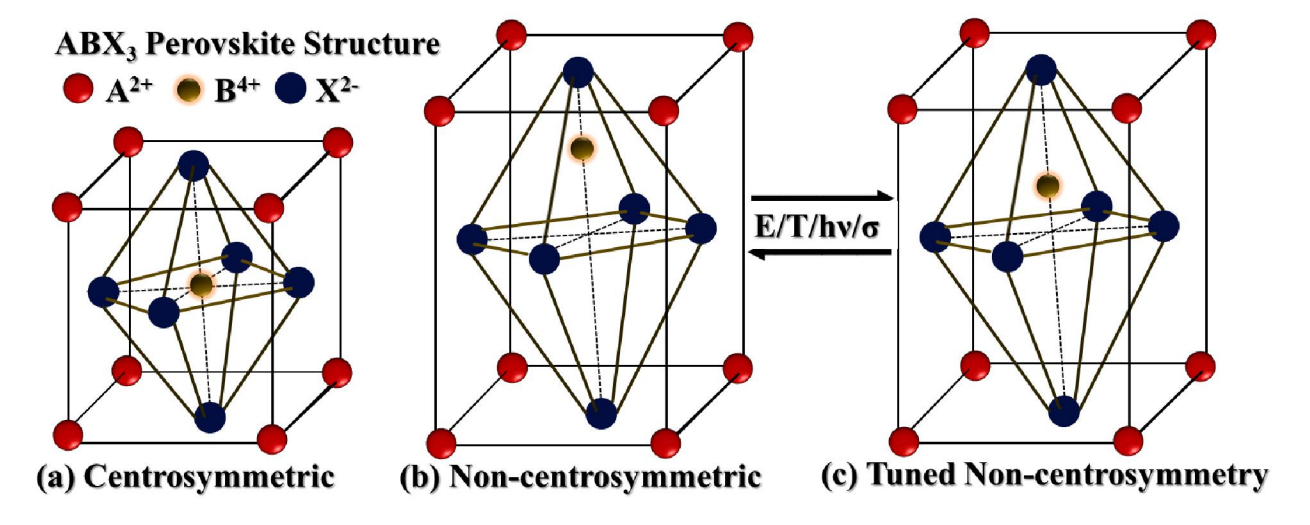


Figure 1

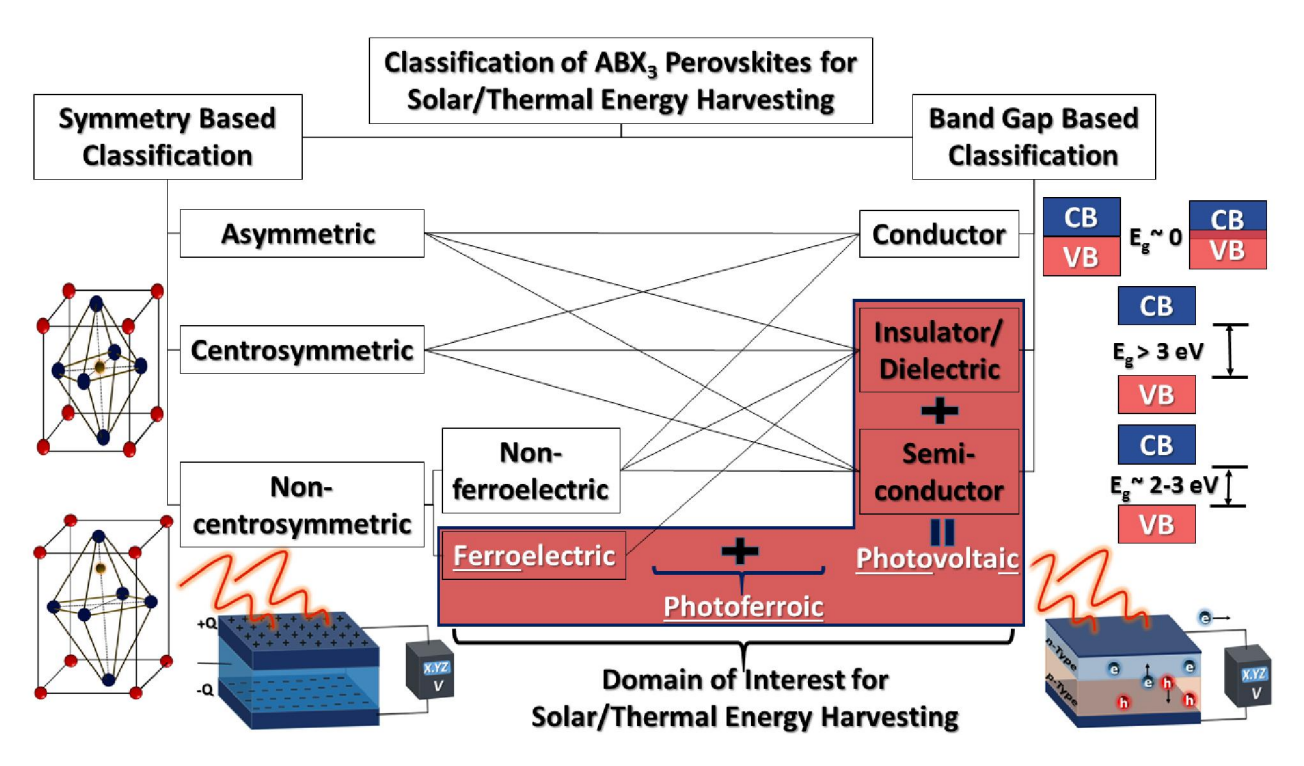


Figure 2

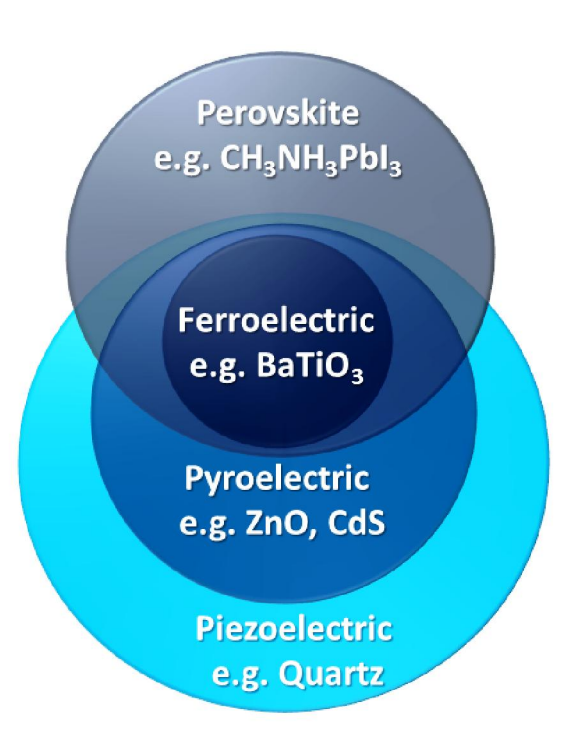


Figure 3

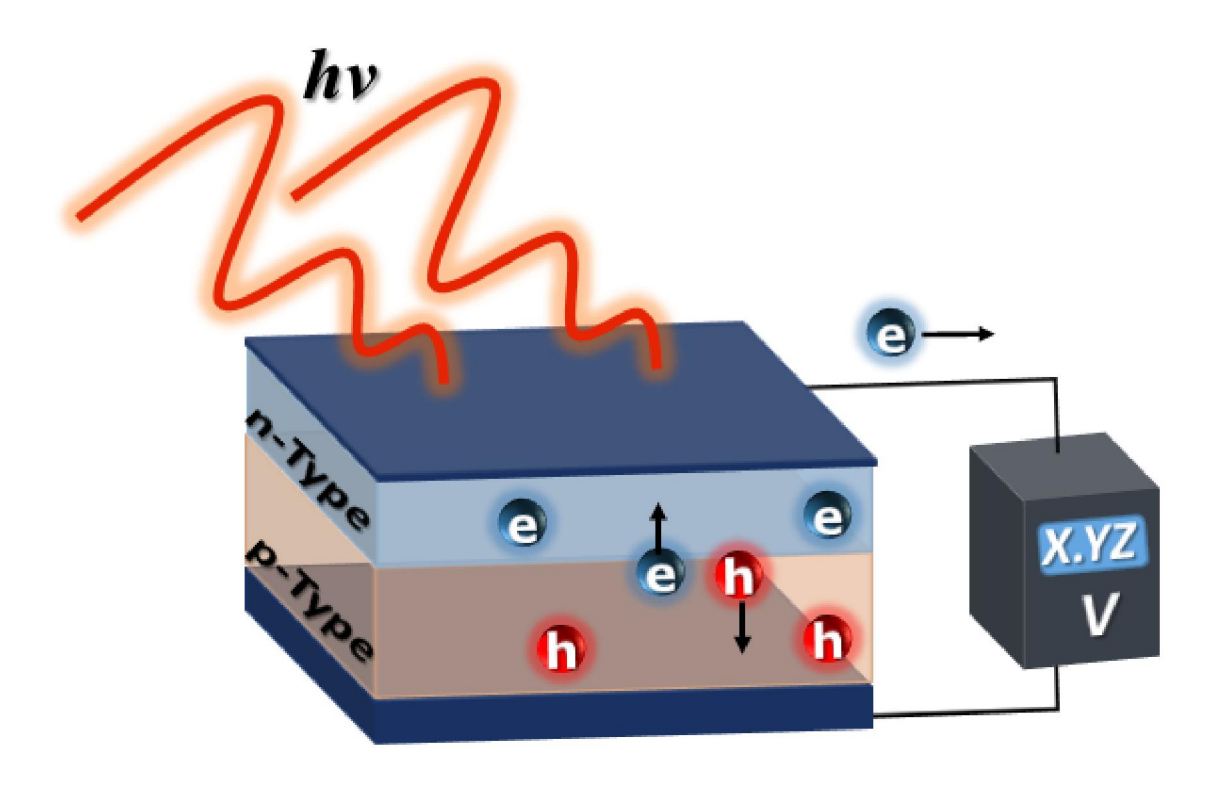


Figure 4

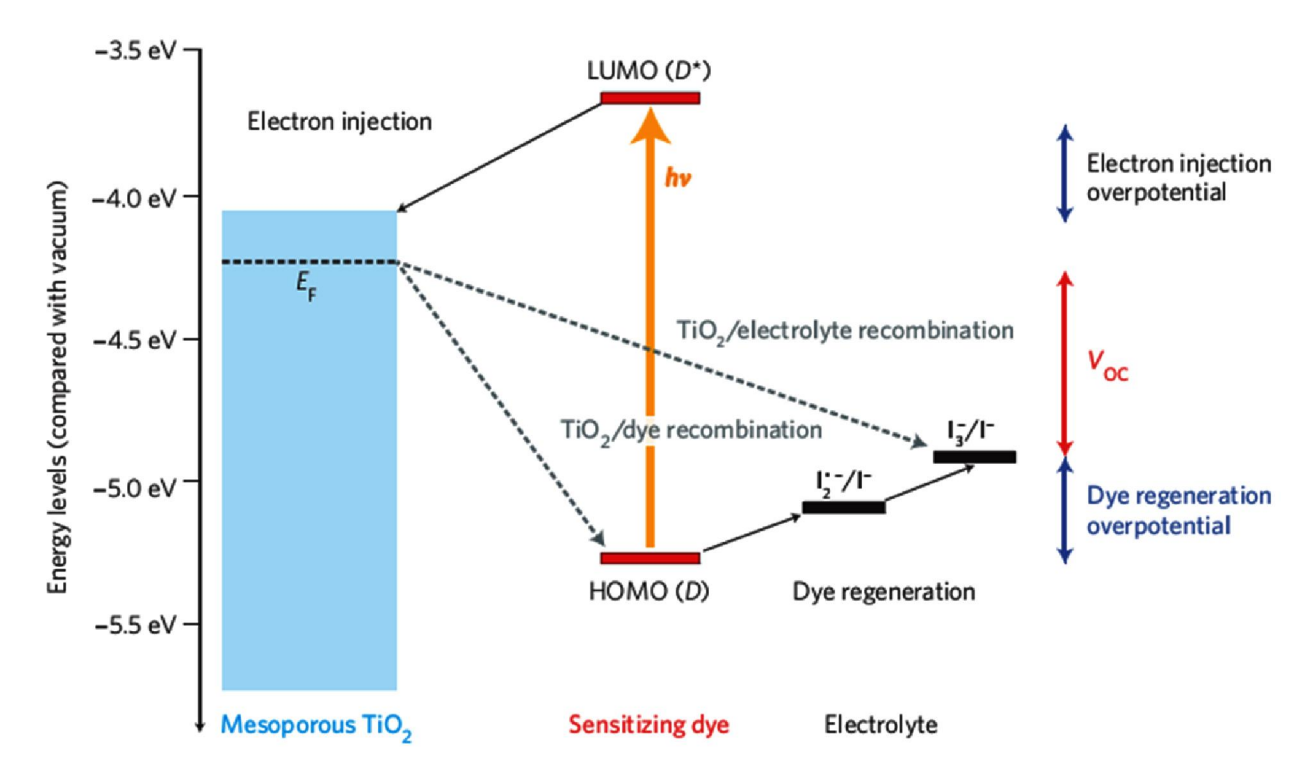


Figure 5

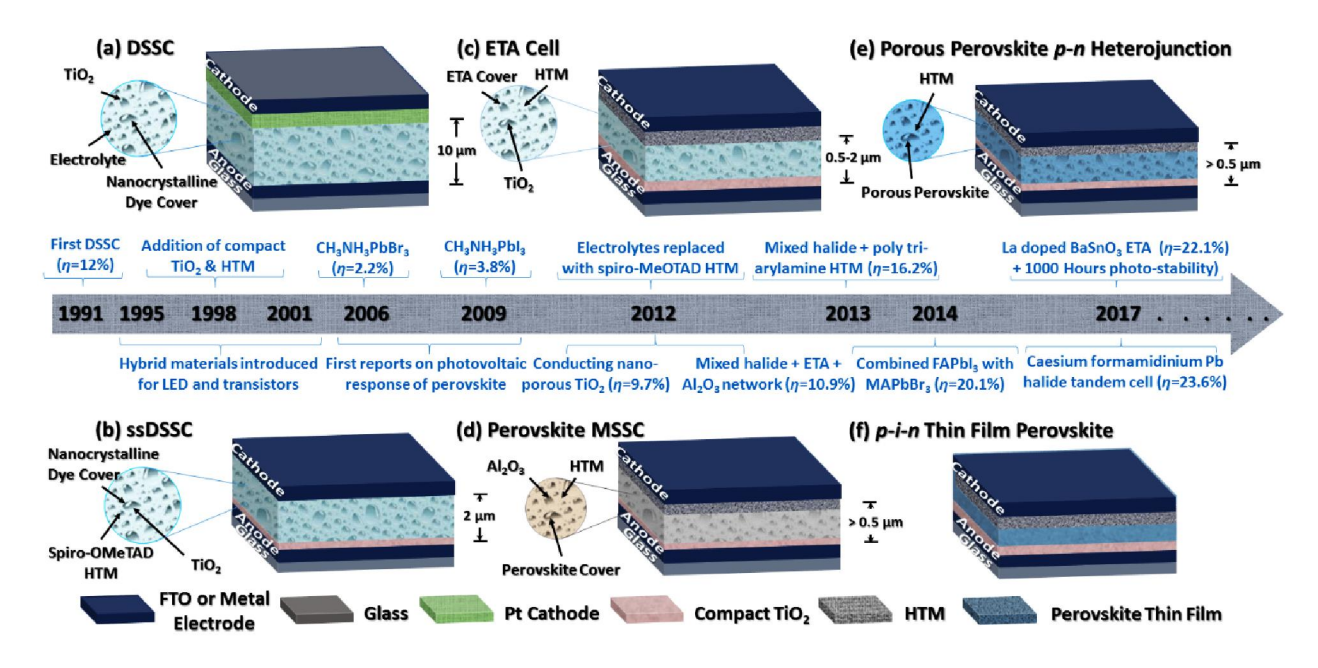


Figure 6

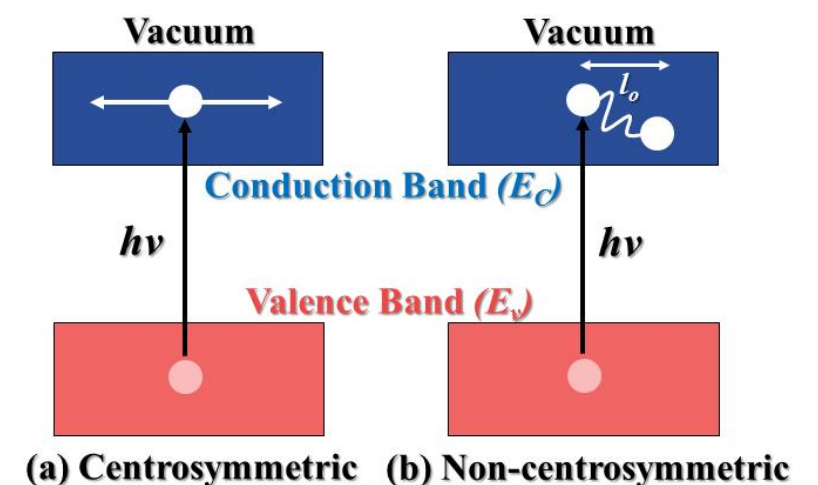


Figure 7

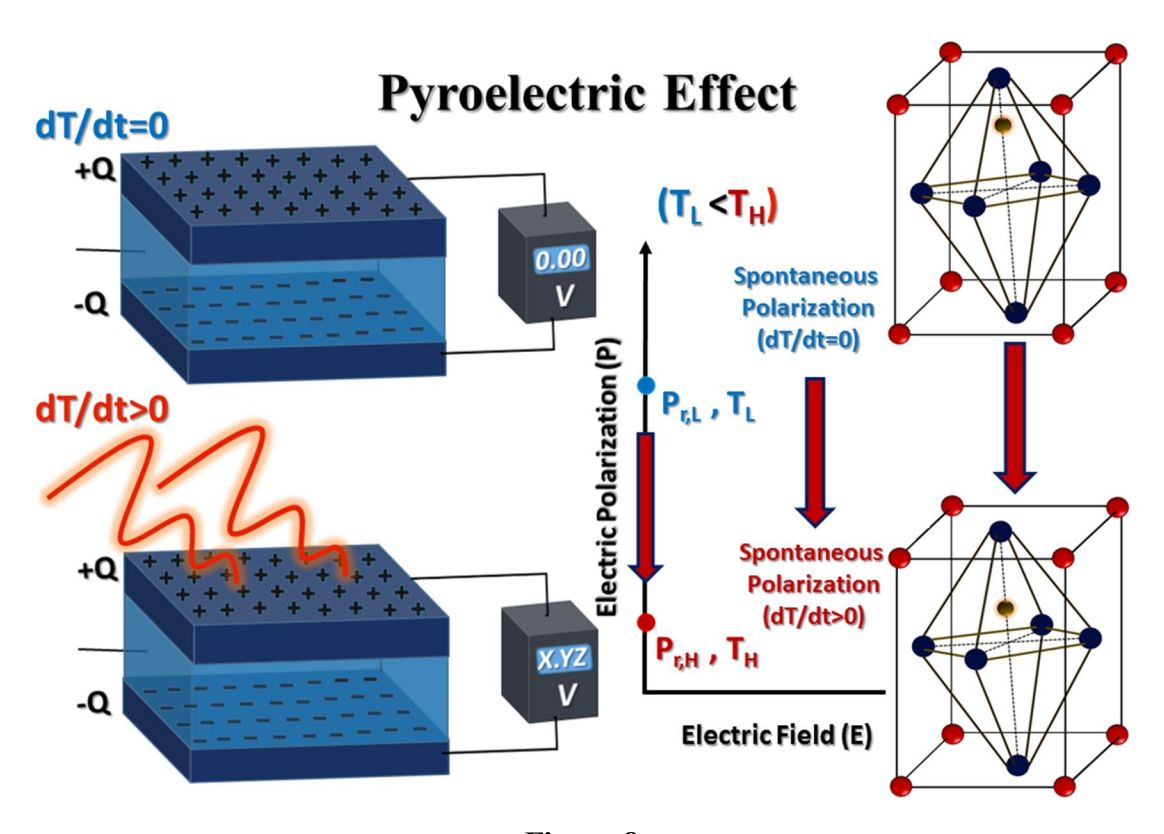


Figure 8

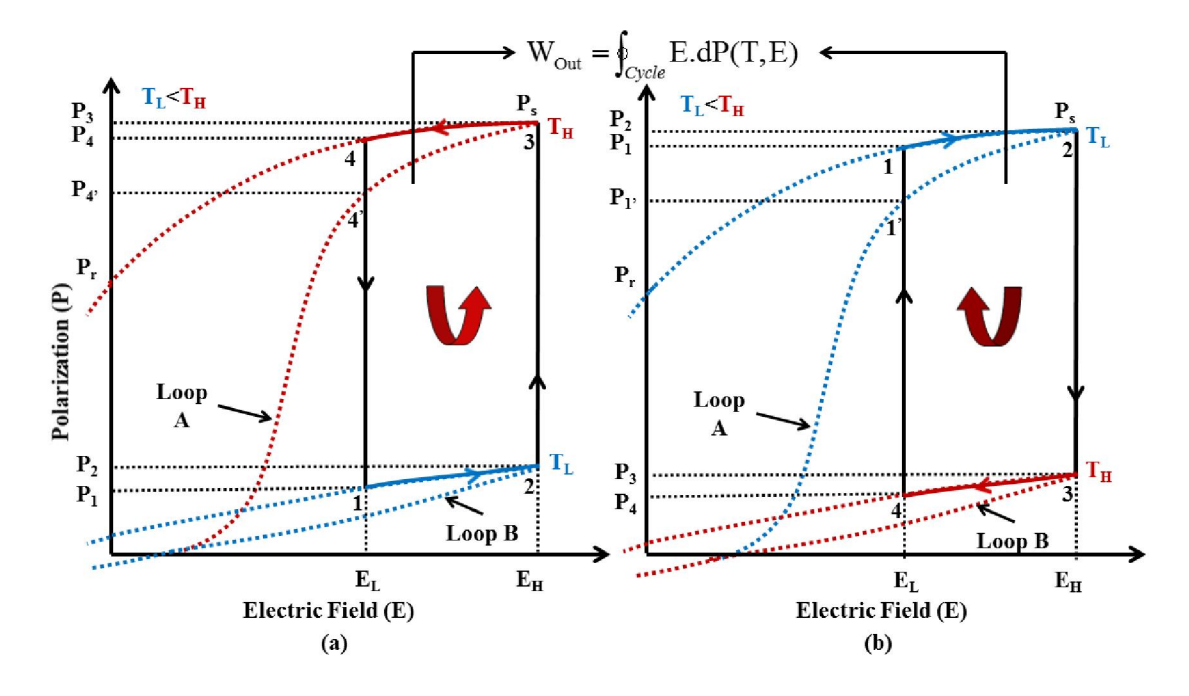


Figure 9

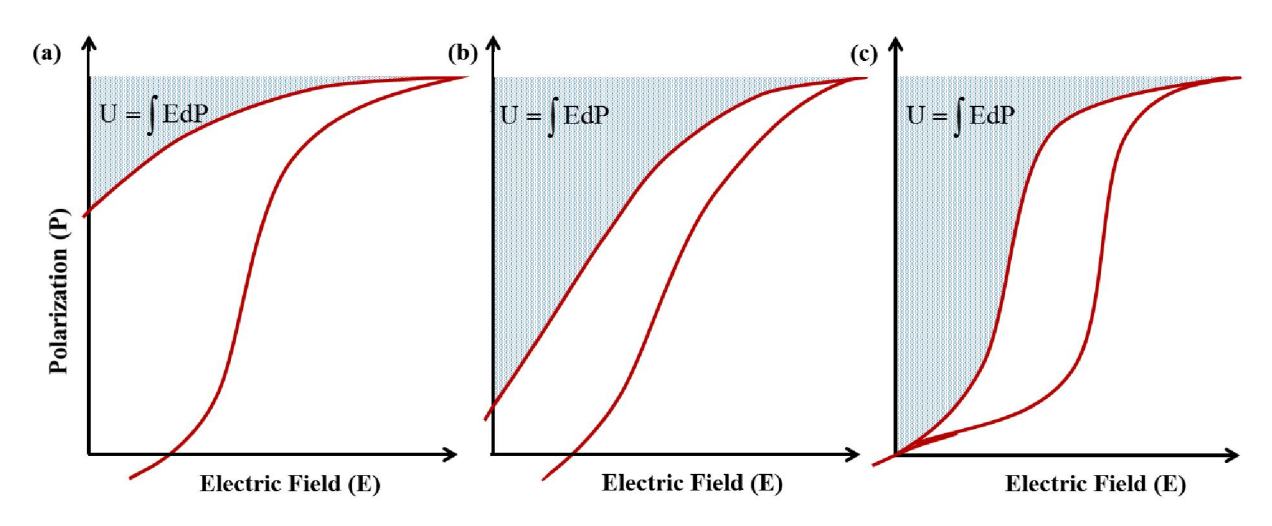


Figure 10